NASA CONTRACTOR REPORT

NASA CR-2023

DEVELOPMENT OF APPROACH CONTROL SYSTEM REQUIREMENTS WITH APPLICATIONS TO A JET TRANSPORT

by Duane T. McRuer and Walter A. Johnson

Prepared by
SYSTEMS TECHNOLOGY, INC.
Hawthorne, Calif. 90250
for Ames Research Center

NATIONAL AERONAUTICS AND SPACE ADMINISTRATION • WASHINGTON, D. C. • MAY 1972

1. Report No.	2. Government Accession No.	3. Recipient's Catalog No.
NASA CR-2023		

4. Title and Subtitle	5. Report Date
Development of Approach Control System Requirements with Applications to a Jet Transport	May 1972
	6. Performing Organization Code

7. Author(s)	8. Performing Organization Report No.
Duane T. McRuer and Walter A. Johnson	TR-182-3
	10. Work Unit No.

9. Performing Organization Name and Address	11. Contract or Grant No.
Systems Technology, Inc. 13766 South Hawthorne Boulevard Hawthorne, California 90250	NAS 2-4892
	13. Type of Report and Period Covered
12. Sponsoring Agency Name and Address	Contractor Report
National Aeronautics & Space Administration Washington, D.C. 20546	14. Sponsoring Agency Code

15. Supplementary Notes

16. Abstract

This report deals with the development of requirements for an approach control system and includes example applications to a jet transport aircraft.

The material presented is divided into two basic parts: a general discussion of approach control requirements, and a specific application resulting in the design of three alternative longitudinal controllers.

The point of view taken is that the essential features of the system structure are the feedbacks themselves, their equalization, and their combinations to create control commands. Use is made of the fact that for successful systems the possible feedback structures are very limited. They derive primarily from guidance, control, and regulation demands; and secondarily from dynamic response characteristics desired by the pilot. From the systems view it is the satisfaction of these requirements that is important rather than the means employed. For this reason, most of the discussion in this report is equally applicable to automatic, manual, or hybrid manual/automatic approach systems.

17. Key Words (Suggested by Author(s))	18. Distribution Statement
aircraft, control, autopilot, manual, approach, jet transport	UNCLASSIFIED-UNLIMITED

19. Security Classif. (of this report)	20. Security Classif. (of this page)	21. No. of Pages	22. Price*
UNCLASSIFIED	UNCLASSIFIED	66	3.00

*For sale by the National Technical Information Service, Springfield, Virginia 22151

1. Landing simulation
2. Instrument Landing systems
3. Automatic pilots
4. Flight simulation

FOREWORD

The research reported here was performed under Contract NAS2-4892 between Systems Technology, Inc., Hawthorne, California, and the National Aeronautics and Space Administration. The NASA project monitor was successively Mel Sadoff and Thomas E. Wempe. The STI Technical Director was Duane T. McRuer, and the Project Engineer was Walter A. Johnson.

The authors would like to express their gratitude to Fred Alex for his fine work on this project.

ABSTRACT

This report deals with the development of requirements for an approach control system and includes example applications to a jet transport aircraft. All of the techniques used have been known for some time, but the process of going from a list of guidance and control requirements to a system design has not been well documented in the past.

The material presented is divided into two basic parts: a general discussion of approach control requirements, and a specific application resulting in the design of three alternative longitudinal controllers.

The point of view taken is that the essential features of the system structure are the feedbacks themselves, their equalization, and their combinations to create control commands. Use is made of the fact that for successful systems the possible feedback structures are very limited. They derive primarily from guidance, control, and regulation demands; and secondarily from dynamic response characteristics desired by the pilot. From the systems view it is the satisfaction of these requirements that is important rather than the means employed. For this reason, most of the discussion in this report is equally applicable to automatic, manual, or hybrid manual/automatic approach systems.

CONTENTS

FIGURES

TABLES

SECTION I

INTRODUCTION

This report documents the development of requirements for an approach control system and includes example applications to a jet transport aircraft. Although all of the techniques used in this report have been known for some time and in spite of the fact that there have been many pages of explanation devoted to design considerations, the process of going from a list of guidance and control requirements to a system design has not been well documented in the past.

The material presented herein is divided into two basic parts: a general discussion of approach control requirements, and a specific application resulting in the design of three alternative longitudinal controllers. (These three controllers are compared and evaluated in terms of Category II approach success probabilities in Ref. 1.)

A brief discussion is presented next to explain the point of view taken in this report. This will help orient the reader, and will also bring out some of the design ground rules.

In approach and landing operations, the aircraft is but one element in a feedback control system. The essential features of the system structure are the feedbacks themselves, their equalization, and their combinations to create control commands. For successful systems, i.e., systems which demonstrate uniform, reliable, high quality approach and landing performance, the possible feedback structures are very limited. They derive primarily from guidance, control, and regulation demands; and secondarily from dynamic response characteristics desired by the pilot. From the systems view it is the satisfaction of these requirements that is important rather than the means employed. In other words, the feedback loops closed is the central issue whether the closures are accomplished automatically or manually. For this reason, most of the discussion in this report is equally applicable to automatic, manual, or hybrid manual/automatic approach systems. Any differences come at a later stage when the feedback functions required are divided between animate and inanimate controllers and when the

subtle differences between automatic controller and pilot dynamics are taken into account.

Stated verbally, the key guidance and control requirements for low-level approach systems are:

- To establish and maintain the aircraft on a specified spatial pathway or beam (e.g., localizer and glide path);
- To reduce flight path errors to zero in a stable, well damped and rapidly responding manner;
- To establish an equilibrium flight condition;
- To limit the speed or angle of attack excursions from this established equilibrium flight condition.

The regulation requirements are similar, i.e.,

- To maintain the established flight path in the presence of disturbances such as gusts, crosswinds, and wind shears;
- To provide a degree of short-time attitude stability in the presence of disturbances.

These requirements relate primarily to the relatively low frequency path modes of the aircraft/control system. In essence, they define outer control loops involving those vehicle motion quantities which define the desired equilibrium state of motion. More often than not, such outer loops, when closed about unmodified aircraft dynamics, do not result in stable, well-damped, rapidly responding systems. Instead, equalization of either a series or a parallel nature is needed to assist. Parallel equalization is most common and is achieved by the use of inner loops which feed back such quantities as attitude, angular velocity, and sometimes linear acceleration. These inner loops dominate the high frequency characteristics of the aircraft/controller system.

To obtain a better appreciation of just what feedbacks the verbal requirement statements imply, we shall consider in Section II the determination of feedback structures for a simplified lateral approach controller

and a more complex longitudinal controller. This will be followed in Section III by a detailed development and analysis of three successively more complex longitudinal approach control systems. To make the discussion in Section III concrete, a DC-8-like aircraft will be assumed and numerical values will be used throughout.

SECTION II

DEVELOPMENT OF FEEDBACK STRUCTURES

A. LATERAL CONTROL

A simplified lateral approach controller is shown in Fig. 1. The fundamental error signal in the system is the lateral displacement from the beam (y_e). This displacement from the beam is the difference between the beam's lateral displacement (y_c) and the aircraft's lateral displacement (y). The beam displacement (which is the commanded lateral displacement) is the sum of the desired lateral displacement (y_i) and beam noise (n_b). When lateral guidance is provided by a localizer, y_i is the runway centerline, and thus equal to zero; for variable path systems y_i is a path command. Getting back to the error signal, y_e can be converted to an angle (λ) sensed by instruments in the aircraft via a relation involving the range from the localizer transmitter (i.e., without noise, $y_e = R\lambda$).

It is noted that in Fig. 1 the measured lateral position error is contaminated by two kinds of noise. In addition to beam noise, there is receiver noise, n_r. Typically, n_b is used to represent all unwanted inputs which are approximately stationary when represented as lengths (i.e., range-independent noise), and n_r is used to represent noises which are approximately stationary when represented as angles (range-dependent noise). Range-dependent noise includes the effective receiver noise, which tends to have a constant rms value at the output of the receiver and thus represents a larger displacement at the longer ranges. An example of range-independent noise is main beam multipath transmissions. For the localizer these are caused primarily by fixed structures. For the glide slope, changes in ground reflection coefficients due to stratified wet and dry layers in the ground ("fixed" for a particular approach), and other deviations of the ground plane from an ideal reflecting surface are important causes.

The receiving, filtering, gain changing, and other operations are represented in the transfer characteristic G_λ, which has the output δ_λ.

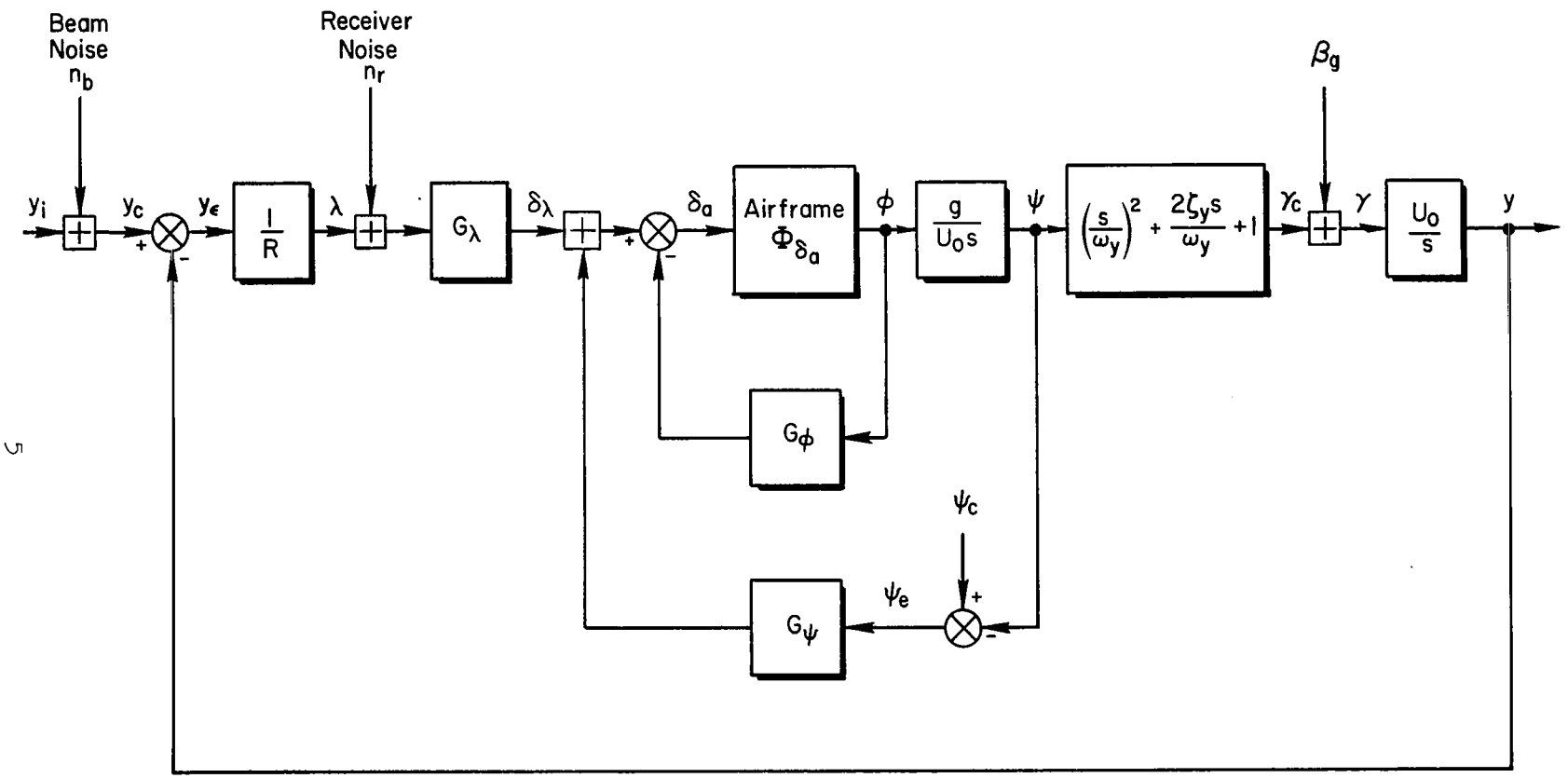

Figure 1. Lateral-Axis Block Diagram of Simplified Approach Controller

This is the effective command to the aircraft/flight control system. The latter comprises the airframe and associated inner-loop controllers.

In the Fig. 1 diagram it is assumed that the aircraft controller feeds back functions of bank angle, φ, and heading, ψ, to modify the basic airframe characteristics. The transfer characteristics G_{φ} and G_{ψ} may be supplied by the pilot and/or an automatic controller. To be explicit we shall assume here that these functions are performed automatically. However, the properties subsequently developed for these transfer characteristics in order that guidance and control requirements be met are also incumbent upon the pilot if he is to play the same role.

In the flight controller block diagram, note that a heading error, ψ_e, is developed by the insertion of a command or bias heading reference signal, ψ_c. Note also that the relationship between heading and bank angle is given by the simplified transfer function, $g/U_o s$. This simplification, as well as that between the flight path angle, γ_c, and heading, are consequences of assuming that the airplane is represented by a three degree of freedom (spiral, roll subsidence) set of simplified equations of motion.* The total aircraft flight path angle, γ, is the sum of that commanded in the flight control system plus an increment due to crosswinds or gusts, $\beta_g = v_g/U_o$. Finally this is converted into a lateral position by multiplying by U_o and integrating.

For the present example we are concerned primarily with path modes; for these, the already simplified system of Fig. 1 can be further simplified if we confine our attention to frequencies less than ω_y. Over this range of frequencies the flight path angle and heading are approximately equal; and, ordinarily, the amplitude ratio of the open-loop roll system ($G_{\varphi}\Phi_{\delta_a}$) is very large. With these simplifications the block diagram becomes that shown in Fig. 2.

---

*These equations are the conventional three-degree-of-freedom lateral set with the simplifying assumption that $(s - Y_v)\beta$ is negligible relative to other side-acceleration quantities. See Section 6.7 of Ref. 2.

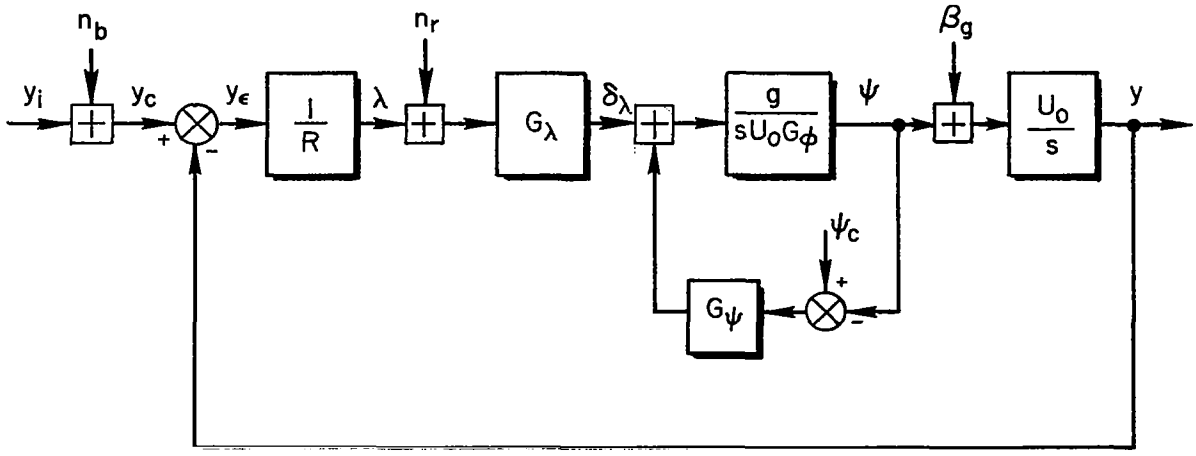

Figure 2. Simplified Lateral-Axis Block Diagram

For this system the Equation of motion is

$$y + \frac{R(t)G_\psi}{U_oG_\lambda} p \left(\frac{U_oG_\varphi}{gG_\psi} p + 1\right) y = y_i + n_b + R(t)n_r + R(t) \frac{G_\psi}{G_\lambda}\left[\psi_c + \left(\frac{U_oG_\varphi}{gG_\psi} p + 1\right)\beta_g\right] \quad (1)$$

where $p = d/dt$. Because the range varies with time, this equation has time varying coefficients, although it is still linear. The range variation gives an increased sensitivity as the aircraft approaches the aiming point. Although a terminal controller which takes advantage of this time variation can be developed to give satisfactory accuracies at the end of the approach, the intrinsic time-varying gain must be offset by a compensating time-varying gain if precision path control is to be maintained throughout the approach. This is done by inserting a range-varying gain as one of the operations in G_λ such that $(1/R)(G_\lambda) = G_y$, where G_y is a constant-coefficient operator. (Altitude or time, which are roughly equivalent to range when on a constant speed approach down a straight path, may be used in place of range.) Then the equation of motion becomes constant coefficient and can be written in Laplace transform notation as

$$\left(\frac{G_\varphi}{g} s^2 + \frac{G_\psi}{U_o} s + G_y\right) y = G_y(y_i + n_b + Rn_r) + G_\psi(\psi_c + \beta_g) + \frac{U_o}{g} G_\varphi s\beta_g \quad (2)$$

We shall study this equation in two ways. First, we will examine the steady-state characteristics in the presence of crosswinds to determine what is needed for windproofing. This shall be followed by consideration of the dynamics, using the characteristic equation, to determine the necessities imposed by path stability and response considerations.

1. Windproofing

To represent a "nearly" steady crosswind, v_c, in the steady state, assume β_g is a step function, $v_c/U_o s$. Then the steady-state characteristics of the system in response to this crosswind will be

$$y(t)\Big]_{t\to\infty} = \lim_{s\to 0} sy(s)$$

$$= \lim_{s\to 0}\left\{\frac{G_\psi}{G_y}(s)\left[s\psi_c(s) + \frac{v_c}{U_o}\right] + \frac{G_\varphi}{gG_y}(s)\, sv_c\right\} \qquad (3)$$

This can be made zero in several ways. For the second term to be zero the form sG_φ/G_y must have a net free s (or higher order) in the numerator. Common possibilities include

$$\frac{sG_\varphi}{G_y}(s) = \frac{sK_\varphi}{K_{\dot{y}}s + K_y} \quad \text{or} \quad \frac{sK_\varphi/(T_\varphi s + 1)}{K_{\dot{y}}s + K_y} \qquad (4)$$

Addition of beam integration (i.e., adding a term $K_{\overline{y}}/s$ to G_y) provides another numerator s to offer further improvement.

For the first term, if $G_\psi/G_y(0)$ is a constant, then a bias step command ψ_c/s must be introduced to the heading reference to just compensate for the crosswind. This requires either iterative trimming operations or precise knowledge of v_c. A better technique is to provide a free s in the numerator of G_ψ/G_y. Commonly used possibilities to achieve this include

$$\frac{G_\psi}{G_y} = \frac{K_{\dot{\psi}}s + K_\psi}{K_{\dot{y}}s + K_y + K_{\bar{y}}/s}$$

or
$$\frac{G_\psi}{G_y} = \frac{K_{\dot{\psi}}s}{K_{\dot{y}}s + K_y} \tag{5}$$

or
$$\frac{G_\psi}{G_y} = 0$$

The type of windproofing actually selected depends to some extent on the feedbacks needed for dynamic control purposes, discussed next.

2. Dynamic Requirements

The effects of feedbacks on the dynamic characteristics of the system can be examined by considering the characteristic equation

$$G_\varphi s^2 + \frac{g}{U_o} G_\psi s + gG_y = 0 \tag{6}$$

The low frequency forms for the controller transfer functions most conventionally used are

$$G_\varphi = \frac{K_\varphi}{T_\varphi s + 1}$$

$$G_\psi = K_\psi \tag{7}$$

$$G_y = K_{\dot{y}}s + K_y + \frac{K_{\bar{y}}}{s}$$

These forms are general and not all are used together. For example, the bank angle will not ordinarily be lagged if a proportional heading K_ψ is present. The characteristic equation with these transfer functions inserted becomes

$$\left[1 + \frac{gT_\varphi}{K_\varphi}\left(K_{\dot{y}} + \frac{K_\psi}{U_o}\right)\right]s^2 + \frac{g}{K_\varphi}\left(K_{\dot{y}} + \frac{K_\psi}{U_o} + T_\varphi K_y\right)s + \frac{g}{K_\varphi}\left(K_y + T_\varphi K_{\bar{y}}\right) + \frac{gK_{\bar{y}}}{K_\varphi s} = 0 \tag{8}$$

Consider, first, Eq. 8 with the path duration integral feedback, $K_{\overline{y}}$, zero. The second-order system resulting represents an approximation to the dominant path mode of the system. For the beam to be followed at all, the constant term must always be present and have a positive value. For the path mode to have any damping the s term must also have a positive coefficient. As seen from Eq. 8 this can be provided by heading (K_ψ), lagged bank angle ($T_\varphi K_y$), path rate ($K_{\dot{y}}$), or by combinations thereof. In addition to providing damping, a heading feedback also provides attitude control that is inimical to mid-frequency windproofing. What happens, of course, is that an aircraft with a tight heading loop, when hit by a crosswind, has a tendency to drift while maintaining a constant heading. This drift will ultimately be brought back by the K_y and $K_{\overline{y}}/s$ feedbacks, but only slowly. Path rate ($\dot{y}$) on the other hand provides superior windproofing at the expense of heading. In the past $\dot{y}$ has been a difficult signal to obtain because of beam noise, so heading has been the typical path damping term. This situation is improving, however, due to the use of complementary filtering and the coming of scanning beams.

Now consider the complete third-order equation. The integral term, $gK_{\overline{y}}/K_\varphi s$, is present to assure steady-state windproofing if K_ψ is not zero (see Eq. 5); it also suppresses steady-state lateral errors caused by crosswind shear. Ordinarily the first-order mode introduced by the integral term has a very long time constant, given approximately by

$$\frac{1}{T_{\overline{y}}} \doteq \frac{K_{\overline{y}}}{K_y + T_\varphi K_{\overline{y}}} \tag{9}$$

The corresponding approximate factors for the dominant second-order path modes are

$$\omega_n \doteq \sqrt{\frac{g(K_y + T_\varphi K_{\overline{y}})}{K_\varphi\left[1 + \frac{gT_\varphi}{K_\varphi}\left(K_{\dot{y}} + \frac{K_\psi}{U_o}\right)\right]}}$$

$$\zeta\omega_n \doteq \frac{g\left(K_{\dot{y}} + \frac{K_\psi}{U_o} + T_\varphi K_y\right)}{2K_\varphi\left[1 + \frac{gT_\varphi}{K_\varphi}\left(K_{\dot{y}} + \frac{K_\psi}{U_o}\right)\right]} \tag{10}$$

In the above discussion we have considered only the path command or stiffening, path trimming, and path damping requirements, as these are fundamental to approach. In addition, there are requirements for attitude control and regulation. A bank angle feedback provides this function in roll. Also, near the touchdown point, tight heading control is needed to assure alignment of the aircraft wheel path with the runway to minimize landing gear sideloads. Just as the heading or path rate is required for damping of the path modes so is bank angle required as an inner loop for heading. Finally, to further improve the total control and regulation precision, an extended flight control system bandwidth is desirable. This is achieved using roll rate feedback to the aileron.

We assume in all of this, of course, that the yaw axis and, in particular, the dutch roll mode and any deleterious adverse yawing effects are taken care of by a suitable set of yaw damper and crossfeed loops. These will entail, in general, washed out yaw rate, side acceleration, and lag-lead aileron crossfeed (or their equivalent) fed to rudder. A block diagram for lateral control during approach incorporating all of these features is shown in Fig. 3. The path damping is provided by a combination of lagged bank angle and $\dot{y}$ derived from a so-called complementary filter. This appropriately mixes and filters $a_{y_{cg}}$, φ, and, perhaps, a smoothed beam rate signal to obtain a broadband approximation to $\dot{y}$.

B. LONGITUDINAL CONTROL

As another concrete example of system feedback selection we will consider a typical longitudinal approach control system.* The total system is shown in Fig. 4. There a distinction is drawn between a measuring subsystem and a control subsystem. The boundary is somewhat

*It is noted in advance that the description of the longitudinal system will differ somewhat from that of the lateral system because the various simplifying assumptions used in the lateral case do not have longitudinal counterparts. Thus the longitudinal example will be more "involved" with algebraic detail, although the same kind of considerations (e.g., path damping, stability, windproofing, etc.) will still apply.

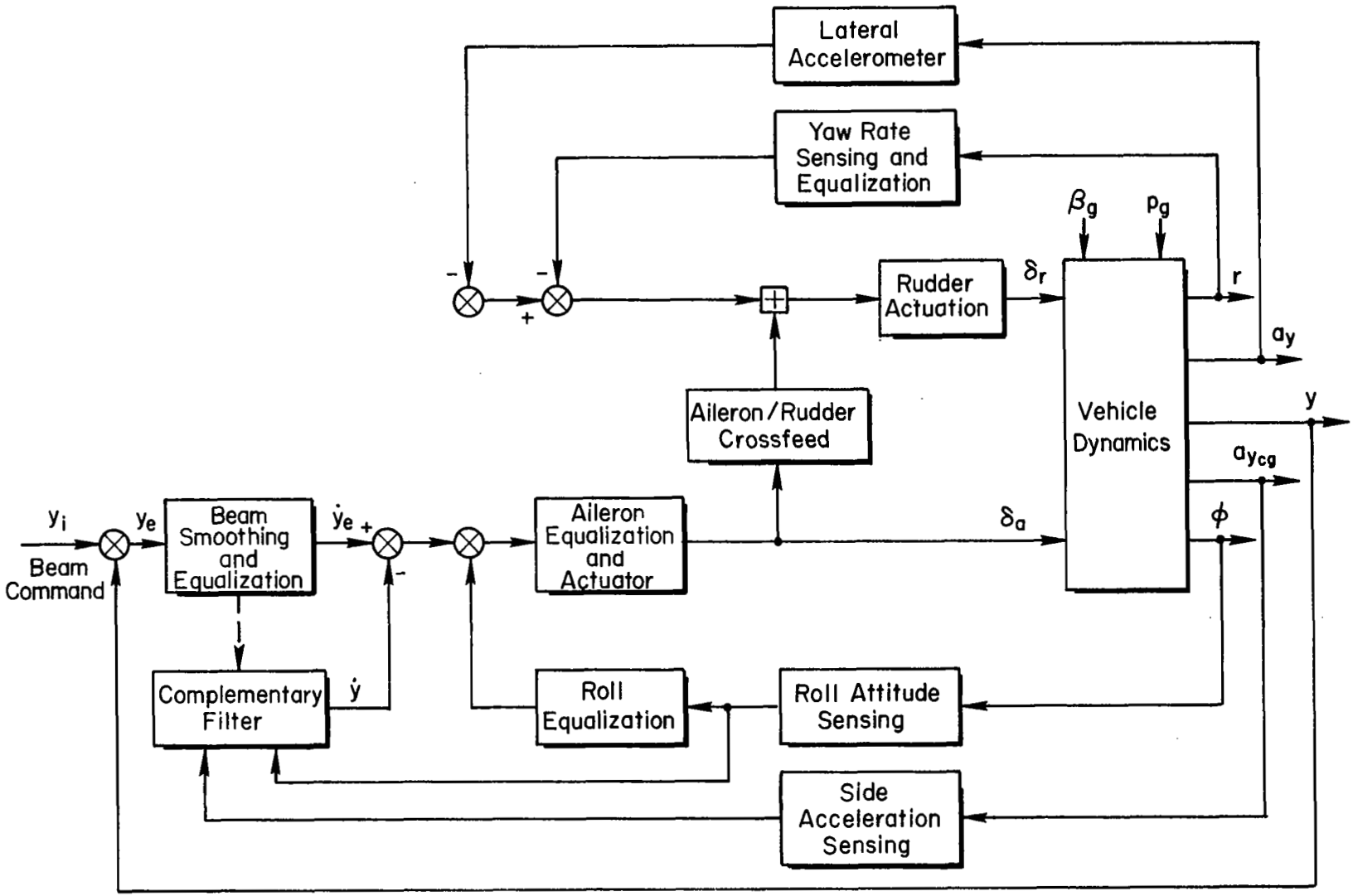

Figure 3 . Block Diagram of Lateral Control for Approach

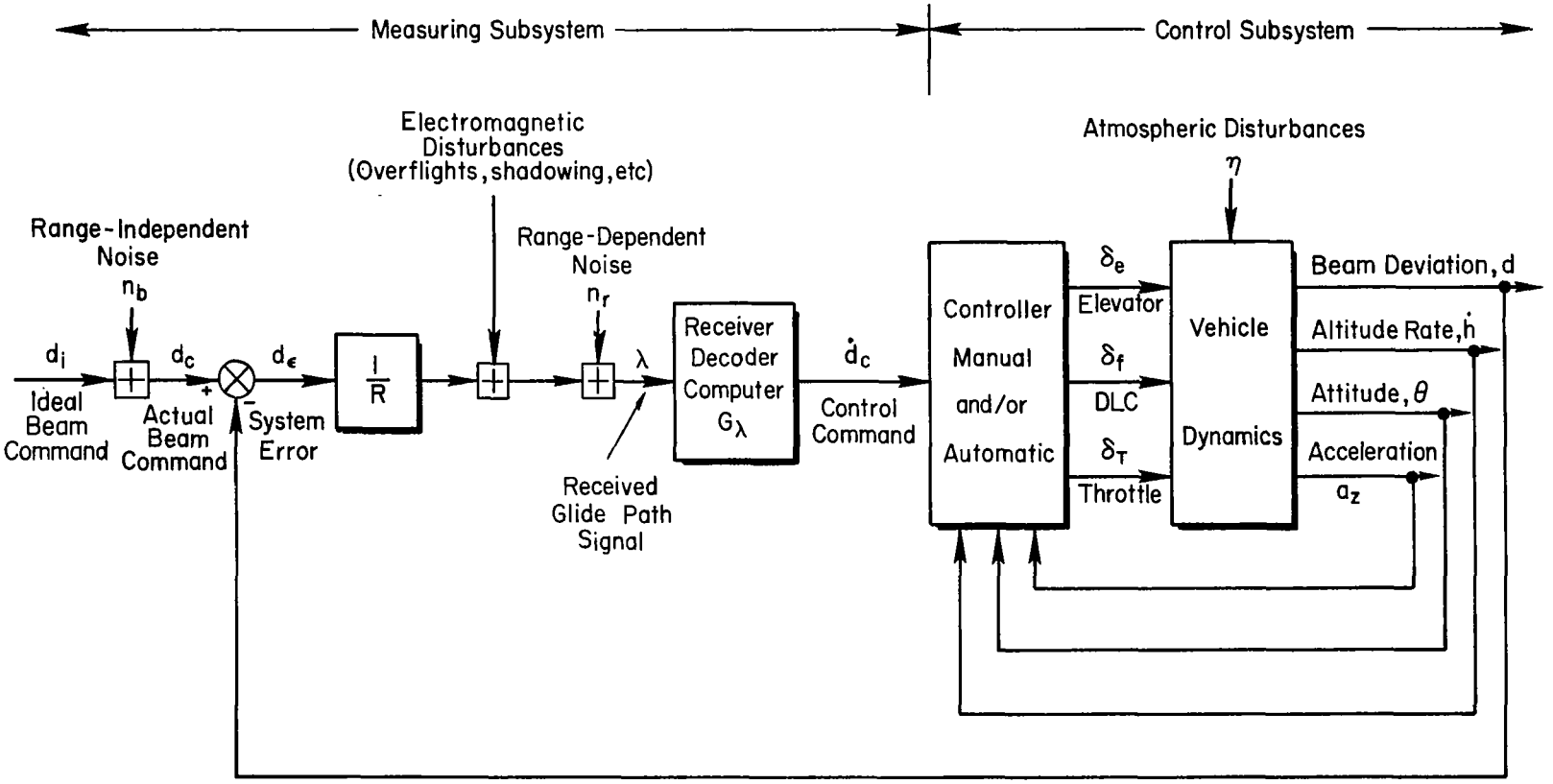

Figure 4 . Measuring and Control System for Vertical Plane Approach and Landing

fuzzy and arbitrary in that certain other vehicle motion characteristics could just as well be included in the measuring subsystem portion. As shown, however, the measuring subsystem emphasizes the ground-to-air transmission of guidance data and the airborne decoding of these data into control system commands.

The measuring subsystem has three important unwanted quantities. Two are the range-dependent and range-independent noises already described for the lateral example. The third unwanted input shown in Fig. 4 is the result of electromagnetic disturbances. These can come from a lead aircraft casting an electromagnetic shadow on following aircraft on the same approach beam pathway, from multipath transmissions of overflying craft (either direct or from side lobes), and so forth.

As Fig. 4 emphasizes the measuring subsystem, so Fig. 5 provides a more detailed breakdown of the control system. Here the measuring subsystem is lumped into the beam smoothing and equalization block. Note that the $\dot{h}_f$ signal, derived from a complementary filter combining barometric and inertial elements, comes from a different path than the deviation from the beam, d. While this $\dot{h}$ signal is shown in the controller in Fig. 4, its location in Fig. 5 indicates that it could just as well be in the measuring subsystem.

In general, the development of an $\dot{h}$-like signal can be accomplished using a combination of the beam rate signal with the outputs of baro and inertial elements in a complementary filtering scheme to reduce the effect of the beam noises on the derived rate. The inertial element can be as simple as an accelerometer or as complex as an inertial navigator. The latter are particularly appropriate for VTOL craft where the longitudinal position can be an important overall landing system loop. Inertial navigation equipment has also been proposed as a means to help reduce the effect of electromagnetic disturbances and noises (when properly combined with the other measuring system elements).

As a simple example of complementary filtering, the composite signal derived from barometric rate of climb and accelerometer sensors, is shown in Fig. 6. For simplicity the higher frequency lags inherent to the system are neglected. The actual rate of climb is $\dot{h}$, and the various n's are

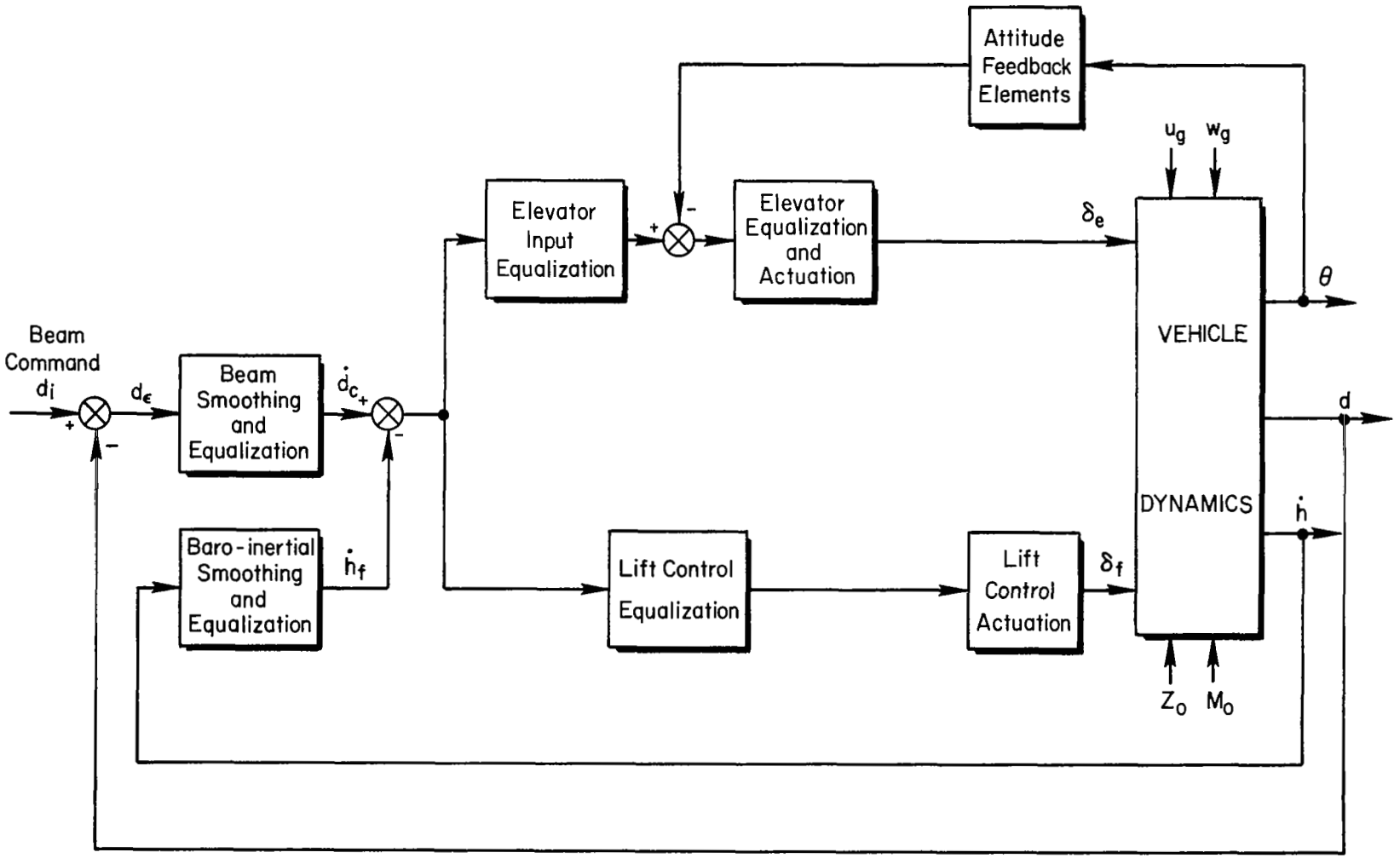

Figure 5. Block Diagram of Longitudinal Control for Approach and Landing

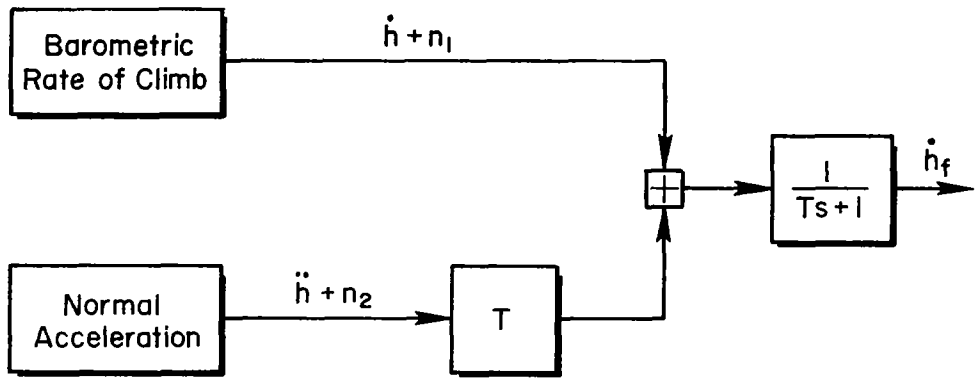

Figure 6. Derivation of Rate-of-Climb Signal

unwanted signals and noises. The composite signal derived, $\dot{h}_f$, is given by

$$\dot{h}_f = \dot{h} + \frac{n_1 + Tn_2}{Ts + 1} \qquad (11)$$

Here, the major signal component is just $\dot{h}$, while the noise terms are heavily filtered. The primary limitation on the time constant, T, is accelerometer noise, which is ordinarily very small at the frequencies of interest here. Consequently, the lag time constant, T, of the composite filter can be made quite large, with attendant reductions in noise. Thus the complementary filter can offer a potent means for the derivation of a good signal from a sum of signals which may be relatively poor individually. It is noted that the present glide slope beam is often too noisy near touchdown to permit its use for path rate computations, even with a complementary filter. This was recognized in the Fig. 5 block diagram, which has only baro and inertial elements called out. However, this situation may change as we gain more experience with Category II ILS, or with future systems. It is also noted that in addition to the noise situation there is a fundamental difference between the $\dot{d}$ and $\dot{h}$ signals. This is that $\dot{d}$ has a steady-state value of zero while $\dot{h}$ has a nonzero steady-state value. The significance of this difference will be presented later.

Returning to describe the remainder of the control system block diagram (Fig. 5), it will be seen that both elevator and direct-lift control are

involved. For the sake of simplicity, a throttle control is not explicitly shown on Fig. 5. As it stands, this block diagram is suitable for manual, automatic, or combined control because the mechanization of the several blocks is not specified. However, the control system is particularized to the point that attitude is fed back only to the elevator. The overall controller equations are given by

$$\delta_e = G_{d_i}^{\delta_e} d_i - (G_d^{\delta_e} d + G_\theta^{\delta_e} \theta) \tag{12}$$

$$\delta_f = G_{d_i}^{\delta_f} d_i - G_d^{\delta_f} d \tag{13}$$

Here, each G is a shorthand notation for the product of all the transfer functions in the blocks between the subscript variable and the superscript variable. For example, $G_{d_i}^{\delta_e}$ is the product of the transfer functions for the blocks labeled: Beam Smoothing and Equalization, Elevator Input Equalization, and Elevator Equalization and Actuation — in short, everything between d_i and δ_e Similarly, $G_{d_i}^{\delta_f}$ will be the product of the transfer functions for the blocks: Beam Smoothing and Equalization, Lift Control Equalization, and Lift Control Actuation. Using this notation the complete closed-loop approach system equations are given below.

$$d = \frac{\left[G_{d_i}^{\delta_e} N_{\delta_e}^{\dot{d}} + G_{d_i}^{\delta_f}(N_{\delta_f}^{\dot{d}} + G_\theta^{\delta_e} N_{\delta_e}^{\theta\,\dot{d}}{}_{\delta_f})\right] d_i + \sum_\eta (N_\eta^{\dot{d}} + G_\theta^{\delta_e} N_{\eta\delta_e}^{\dot{d}\theta}) \eta + G_{n_e}^{\delta_e} N_{\delta_e}^{\dot{d}} n_e + G_{n_f}^{\delta_f}(N_{\delta_f}^{\dot{d}} + G_\theta^{\delta_e} N_{\delta_e}^{\theta\,\dot{d}}{}_{\delta_f}) n_f}{s\Delta + sG_\theta^{\delta_e} N_{\delta_e}^{\theta} + G_d^{\delta_e} N_{\delta_e}^{\dot{d}} + G_d^{\delta_f}(N_{\delta_f}^{\dot{d}} + G_\theta^{\delta_e} N_{\delta_e\delta_f}^{\theta\,\dot{d}})} \tag{14}$$

$$\theta = \frac{\left[G_{d_i}^{\delta_e}(sN_{\delta_e}^{\theta} + G_d^{\delta_f} N_{\delta_f\delta_e}^{\dot{d}\,\theta}) + G_{d_i}^{\delta_f}(sN_{\delta_f}^{\theta} + G_d^{\delta_e} N_{\delta_f\delta_e}^{\theta\,\dot{d}})\right] d_i + \sum_\eta (sN_\eta^{\theta} + G_d^{\delta_f} N_{\eta\delta_f}^{\theta\dot{d}} + G_d^{\delta_e} N_{\eta\delta_e}^{\theta\dot{d}}) \eta + G_{n_e}^{\delta_e}(sN_{\delta_e}^{\theta} + G_d^{\delta_f} N_{\delta_f\delta_e}^{\dot{d}\,\theta}) n_e + G_{n_f}^{\delta_f}(sN_{\delta_f}^{\theta} + G_d^{\delta_e} N_{\delta_f\delta_e}^{\theta\,\dot{d}}) n_f}{s\Delta + sG_\theta^{\delta_e} N_{\delta_e}^{\theta} + G_d^{\delta_e} N_{\delta_e}^{\dot{d}} + G_d^{\delta_f}(N_{\delta_f}^{\dot{d}} + G_\theta^{\delta_e} N_{\delta_e\delta_f}^{\theta\,\dot{d}})} \tag{15}$$

η = w_g, u_g

Δ = Airframe-alone characteristic function

$N^{\theta}_{\delta_e}$, $N^{\dot{d}}_{\delta_f}$, etc. = Airframe-alone transfer function numerators

$N^{\theta\,\dot{d}}_{\delta_e\delta_f}$, $N^{\theta\dot{d}}_{\eta\delta_f}$, etc. = Airframe-alone coupling numerators

n_e = Lumped noise effectively acting in elevator channel

n_f = Lumped noise effectively acting in flap (DLC) channel

Equations 14 and 15 combine the controller equations with those of the vehicle, which is characterized by the transfer function numerators, coupling numerators, and characteristic function. These are summarized in Table 1. Notice that the trim and atmospheric disturbances are denoted by a general disturbance input, η, and that the noises are lumped into an n_e for elevator, and an n_f for the DLC channels respectively. Equations for other aircraft motion quantities, such as u, can be obtained from Eq. 15 simply by replacing the θ superscripts in the numerator by the new variable.

TABLE 1

LONGITUDINAL EQUATIONS, TRANSFER FUNCTIONS, AND COUPLING NUMERATORS

Equations of Motion

$$\begin{bmatrix} s-X_u & -X_w & g\cos\Theta_o \\ -Z_u & s-Z_w & -U_o s+g\sin\Theta_o \\ -M_u & -(M_{\dot{w}}s+M_w) & s(s-M_q) \end{bmatrix} \begin{bmatrix} u \\ w \\ \theta \end{bmatrix} = \begin{bmatrix} X_{\delta_e} & X_{\delta_T} & X_{\delta_f} & -X_\eta \\ Z_{\delta_e} & Z_{\delta_T} & Z_{\delta_f} & -Z_\eta \\ M_{\delta_e} & M_{\delta_T} & M_{\delta_f} & -M_\eta \end{bmatrix} \begin{bmatrix} \delta_e \\ \delta_T \\ \delta_f \\ \eta \end{bmatrix}$$

$$\dot{d} = -w + U_o\theta$$

$$\dot{h} = -U_o \sin\Theta_o - w\cos\Theta_o + u\sin\Theta_o + U_o\cos\Theta_o\theta$$

TABLE 1 (Continued)

Characteristic Function (See note at end of Table)

$$\Delta_{long} = (A_\Delta s^4 + B_\Delta s^3 + C_\Delta s^2 + D_\Delta s + E_\Delta)$$

$$A_\Delta = 1$$

$$B_\Delta = -(M_q + Z_w + U_o M_{\dot{w}} + X_u)$$

$$C_\Delta = M_q Z_w - U_o M_w + X_u(M_q + Z_w + U_o M_{\dot{w}}) - X_w Z_u + g M_{\dot{w}} \sin \Theta_o$$

$$D_\Delta = -X_u(Z_w M_q - U_o M_w) - M_u U_o X_w + M_q Z_u X_w + g \cos \Theta_o(M_u + Z_u M_{\dot{w}}) + g \sin \Theta_o(M_w - X_u M_{\dot{w}})$$

$$E_\Delta = g \cos \Theta_o(M_w Z_u - M_u Z_w) + g \sin \Theta_o(M_u X_w - M_w X_u)$$

Numerators

$$N_\delta^{\dot{d}} = A_\delta^{\dot{d}} s^3 + B_\delta^{\dot{d}} s^2 + C_\delta^{\dot{d}} s + D_\delta^{\dot{d}}$$

$$A_\delta^{\dot{d}} = -Z_\delta$$

$$B_\delta^{\dot{d}} = Z_\delta(U_o M_{\dot{w}} + M_q + X_u) - X_\delta Z_u$$

$$C_\delta^{\dot{d}} = U_o[M_{\dot{w}}(X_\delta Z_u - Z_\delta X_u) + (Z_\delta M_w - Z_w M_\delta)] + M_q(Z_u X_\delta - X_u Z_\delta) + g M_\delta \sin \theta$$

$$D_\delta^{\dot{d}} = U_o[X_\delta(Z_u M_w - M_u Z_w) - Z_\delta(M_w X_u - X_w M_u) - M_\delta(X_w Z_u - Z_w X_u)] + g \cos \theta_o(Z_u M_\delta - M_u Z_\delta) + g \sin \theta_o(M_u X_\delta - X_u M_\delta)$$

$$N_\eta^{\dot{d}} = A_\eta^{\dot{d}} s^3 + B_\eta^{\dot{d}} s^2 + C_\eta^{\dot{d}} s + D_\eta^{\dot{d}}$$

$$A_\eta^{\dot{d}} = +Z_\eta$$

$$B_\eta^{\dot{d}} = -Z_\eta(U_o M_{\dot{w}} + M_q + X_u) + X_\eta Z_u$$

$$C_\eta^{\dot{d}} = U_o[M_{\dot{w}}(Z_\eta X_u - X_\eta Z_u) + (M_\eta Z_w - Z_\eta M_w)] + M_q(X_u Z_\eta - Z_u X_\eta) - g M_\eta \sin \theta_o$$

$$D_\eta^{\dot{d}} = U_o[X_\eta(M_u Z_w - Z_u M_w) + Z_\eta(M_w X_u - X_w M_u) + M_\eta(X_w Z_u - Z_w X_u)] + g \cos \theta_o(Z_\eta M_u - Z_u M_\eta) + g \sin \theta_o(X_u M_\eta - M_u X_\eta)$$

TABLE 1 (Concluded)

$$N_\delta^\theta = A_\delta^\theta s^2 + B_\delta^\theta s + C_\delta^\theta$$

$$A_\delta^\theta = Z_\delta M_{\dot{w}} + M_\delta$$

$$B_\delta^\theta = X_\delta(M_{\dot{w}} Z_u + M_u) + Z_\delta(M_w - M_{\dot{w}} X_u) - M_\delta(Z_w + X_u)$$

$$C_\delta^\theta = X_\delta(M_w Z_u - M_u Z_w) + Z_\delta(M_u X_w - M_w X_u) + M_\delta(Z_w X_u - X_w Z_u)$$

$$N_\eta^\theta = A_\eta^\theta s^2 + B_\eta^\theta s + C_\eta^\theta$$

$$A_\eta^\theta = -(Z_\eta M_{\dot{w}} + M_\eta)$$

$$B_\eta^\theta = + [-X_\eta(M_{\dot{w}} Z_u + M_u) - Z_\eta(M_w - M_{\dot{w}} X_u) + M_\eta(Z_w + X_u)]$$

$$C_\eta^\theta = -X_\eta(M_w Z_u - M_u Z_w) - Z_\eta(M_u X_w - M_w X_u) - M_\eta(Z_w X_u - X_w Z_u)$$

Coupling Numerators

$$N_{\delta_e \delta_f}^{\theta\, \dot{d}} = A_{\delta_e \delta_f}^{\theta\, \dot{d}} s + B_{\delta_e \delta_f}^{\theta\, \dot{d}}$$

$$A_{\delta_e \delta_f}^{\theta\, \dot{d}} = (Z_{\delta_e} M_{\delta_f} - Z_{\delta_f} M_{\delta_e})$$

$$B_{\delta_e \delta_f}^{\theta\, \dot{d}} = X_u(Z_{\delta_f} M_{\delta_e} - Z_{\delta_e} M_{\delta_f}) - Z_u(X_{\delta_f} M_{\delta_e} - X_{\delta_e} M_{\delta_f}) + M_u(X_{\delta_f} Z_{\delta_e} - X_{\delta_e} Z_{\delta_f})$$

$$N_\eta^{\dot{d}\, \theta}{}_\delta = A_\eta^{\dot{d}\, \theta}{}_\delta s + B_\eta^{\dot{d}\, \theta}{}_\delta$$

$$A_\eta^{\dot{d}\, \theta}{}_\delta = Z_\eta M_\delta - M_\eta Z_\delta$$

$$B_\eta^{\dot{d}\, \theta}{}_\delta = -X_u(Z_\eta M_\delta - M_\eta Z_\delta) + Z_u(X_\eta M_\delta - M_\eta X_\delta) - M_u(X_\eta Z_\delta - Z_\eta X_\delta)$$

Note that some of the transfer function numerators are defined in terms of error rate (rather than error) in order to avoid the confusion that can arise from transfer function numerators having denominators. Thus, the transfer function for $\dot{d}/\delta_e$ is defined to be $N_{\delta_e}^{\dot{d}}/\Delta_{long}$, and the transfer function for d/δ_e is $N_{\delta_e}^{\dot{d}}/s\Delta_{long}$. By <u>not</u> using the symbol $N_{\delta_i}^{\dot{d}}$, all numerators ($N_{\delta_i}^{j}$) remain "pure" polynomials (rather than ratios of polynomials).

Having described the control system block diagram (Fig. 5), and defined the airframe transfer functions (Table 1), it is now appropriate to give a "verbal" description of the fundamental guidance and control requirements for the longitudinal approach system.

- Guidance Requirements

  The aircraft must follow the beam commands

- Regulation Requirements
  - The aircraft should be maintained close to the beam in the presence of winds, gust disturbances, internal biases in the equipment, measuring system noise, etc.
  - Aircraft attitude should be kept stable and "solid", i.e., relatively constant, in the presence of the disturbance environment.

- Implied (Mechanization-based) Requirement

  Elevator must be used for trim adjustments (i.e., DLC is <u>not</u> to be saturated due to trim changes)

Most of these qualitative requirements can readily be translated into required feedbacks by considering certain steady-state aspects of the system equations, followed by simple stability and response arguments. We shall consider the steady-state features first.

Guidance Requirement

The most fundamental guidance requirement is that the aircraft acquire the beam when the system is engaged. In other words, the deviation from the beam, d, must ultimately become zero when the system "input" is an initial condition, d(0+). The response transform of an nth order system with characteristic function

$$\Delta_{sys} = s^n + a_1 s^{n-1} + \cdots + a_{n-1} s + a_n \tag{16}$$

to an initial condition of position, d(0+), is readily shown to be

$$d(s) = \frac{(s^{n-1} + a_1 s^{n-2} + \cdots + a_{n-1}) d(0+)}{s^n + a_1 s^{n-1} + \cdots + a_{n-1} s + a_n} \tag{17}$$

Assuming that the final value theorem holds,

$$\lim_{t\to\infty} d(t) = \lim_{s\to 0} sd(s)$$

$$= \lim_{s\to 0} s \frac{(s^{n-1} + a_1 s^{n-2} + \cdots + a_{n-1})d(0+)}{s^n + a_1 s^{n-1} + \ldots + a_{n-1}s + a_n} \tag{18}$$

which will be zero only when $a_n \neq 0$. Consequently the characteristic function must contain a constant term for the system to acquire the beam. The characteristic function is

$$\Delta_{sys} = s\Delta_{long} + sG_\theta^{\delta_e} N_{\delta_e}^\theta + G_d^{\delta_e} N_{\delta_e}^{\dot{d}} + G_d^{\delta_f}(N_{\delta_f}^{\dot{d}} + G_\theta^{\delta_e} N_{\delta_e \delta_f}^{\theta\,\dot{d}}) \tag{19}$$

As s approaches zero, $s\Delta_{long}$, $sN_{\delta_e}^\theta$, $N_\delta^{\dot{d}}$, and $N_{\delta_e\delta_f}^{\theta\,\dot{d}}$ approach sE_Δ, $sC_{\delta_e}^\theta$, $D_\delta^{\dot{d}}$, and $B_{\delta_e\delta_f}^{\theta\,\dot{d}}$, respectively. So, as s approaches zero in Eq. 19,

$$\lim_{s\to 0} \Delta_{sys} = \lim_{s\to 0} \left\{ s\left[E_\Delta + G_\theta^{\delta_e}(s) C_{\delta_e}^\theta\right] + G_d^{\delta_e}(s) D_{\delta_e}^{\dot{d}} + G_d^{\delta_f}(s)\left[D_{\delta_f}^{\dot{d}} + G_\theta^{\delta_e} B_{\delta_e\delta_f}^{\theta\,\dot{d}}\right] \right\} \tag{20}$$

For the attitude control to be significant in this expression attitude feedback, $G_\theta^{\delta_e}$, would have to contain an integral term. This would conflict with the desire to drive d to zero for other inputs. Consequently $G_\theta^{\delta_e}(0)$ will be made either a constant or zero. Also, for reasons which will be described later, the DLC control of path deviation, $G_d^{\delta_f}$, should have one more free s than the elevator/path deviation transfer function, $G_d^{\delta_e}$. This leaves the $G_d^{\delta_e}(s) D_{\delta_e}^{\dot{d}}$ term, which will satisfy our need for a constant in Δ_{sys} if $G_d^{\delta_e}$ contains a proportional ($K_d^{\delta_e}$) term. Thus, all of this justifies the intuitively obvious requirement for a proportional feedback of path deviation to achieve static stability relative to the beam.

Another guidance requirement is that the system follow guidance commands, d_i. These might arise from a one-step beam scheme or even a higher order curvature command in more advanced systems.

In following guidance commands, d_i, the error d_ϵ is given by

$$d_\epsilon = d_i - d$$

$$= \frac{s\Delta + sG_\theta^{\delta_e} N_{\delta_e}^{\theta} + N_{\delta_e}^{\dot{d}}\left(G_d^{\delta_e} - G_{d_i}^{\delta_e}\right) + \left(N_{\delta_f}^{\dot{d}} + G_\theta^{\delta_e} N_{\delta_e \delta_f}^{\theta\,\dot{d}}\right)\left(G_d^{\delta_f} - G_{d_i}^{\delta_f}\right)}{s\Delta + sG_\theta^{\delta_e} N_{\delta_e}^{\theta} + G_d^{\delta_e} N_{\delta_e}^{\dot{d}} + G_d^{\delta_f}\left(N_{\delta_f}^{\dot{d}} + G_\theta^{\delta_e} N_{\delta_e \delta_f}^{\theta\,\dot{d}}\right)} d_i \qquad (21)$$

Letting $G_d^{\delta} = G_{d_i}^{\delta} + Y_d^{\delta}$ for both δ_e and δ_f then gives,

$$d_\epsilon = \frac{s\Delta + sG_\theta^{\delta_e} N_{\delta_e}^{\theta} + Y_d^{\delta_e} N_{\delta_e}^{\dot{d}} + Y_d^{\delta_f}\left(N_{\delta_f}^{\dot{d}} + G_\theta^{\delta_e} N_{\delta_e \delta_f}^{\theta\,\dot{d}}\right)}{s\Delta + sG_\theta^{\delta_e} N_{\delta_e}^{\theta} + G_d^{\delta_e} N_{\delta_e}^{\dot{d}} + G_d^{\delta_f}\left(N_{\delta_f}^{\dot{d}} + G_\theta^{\delta_e} N_{\delta_e \delta_f}^{\theta\,\dot{d}}\right)} d_i \qquad (22)$$

If the commanded path is given by a power series in time, i.e.,

$$d_i(t) = d_1 + d_2 t + d_3 t^2 + \cdots \qquad (23)$$

then

$$d_i(s) = \frac{d_1}{s} + \frac{d_2}{s^2} + \frac{2d_3}{s^3} + \cdots \qquad (24)$$

and the lowest order term in s will be $(n-1)!d_n/s^n$. Using the final value theorem,

$$\epsilon_{\text{steady state}} = \lim_{s \to 0}\left[\left\{\frac{s\Delta + sG_\theta^{\delta_e} N_{\delta_e}^{\theta} + Y_d^{\delta_e} N_{\delta_e}^{\dot{d}} + Y_d^{\delta_f}\left(N_{\delta_f}^{\dot{d}} + G_\theta^{\delta_e} N_{\delta_e \delta_f}^{\theta\,\dot{d}}\right)}{s\Delta + sG_\theta^{\delta_e} N_{\delta_e}^{\theta} + G_d^{\delta_e} N_{\delta_e}^{\dot{d}} + G_d^{\delta_f}\left(N_{\delta_f}^{\dot{d}} + G_\theta^{\delta_e} N_{\delta_e \delta_f}^{\theta\,\dot{d}}\right)}\right\} \frac{(n-1)!d_n}{s^{n-1}}\right] \qquad (25)$$

For the system to follow a command path of nth order the numerator of the curly bracketed expression in Eq. 25 must contain a free s^n. From the sketch it is apparent that a system which is stabilized on the first segment of a two segment glide path system must follow a ramp function in d without steady-state error if it is to successfully transition from path 1 to 2. So a free s^2 is needed in the curly bracketed

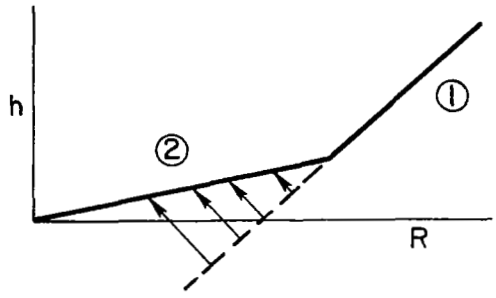

portion of Eq. 25. Using the same limiting properties as in the beam acquisition case,

$$\lim_{s\to 0}\{\ \} = \lim_{s\to 0}\left\{\frac{s\left[E_{\Delta} + G_{\theta}^{\delta_e}(s)C_{\delta_e}^{\theta}\right] + Y_{d}^{\delta_e}(s)D_{\delta_e}^{\dot{d}}}{G_{d}^{\delta_e}(s)D_{\delta_e}^{\dot{d}}}\right\} \tag{26}$$

$Y_d^{\delta_e}$ typically is either zero or contains a single free s, so the total numerator in Eq. 26 has a net free s. Then, to provide the second numerator free s (needed to satisfy the steady-state requirement) the path deviation/elevator transfer function must have an integral term, $K_d^{\delta_e}/s$. This is also obvious intuitively from examination of Fig. 5. There it is plain that a steady-state signal must be developed at the $\dot{d}_c$ point to offset a change in the steady-state output of the Baro-inertial Smoothing and Equalization block.

Regulation Requirements

The path deviation response to an external disturbance η is given by

$$d_{\eta} = \frac{N_{\eta}^{\dot{d}} + G_{\theta}^{\delta_e}N_{\eta}^{\dot{d}}\,{}^{\theta}_{\delta_e}}{\Delta_{sys}}\,\eta \tag{27}$$

where η may be a w_g or u_g wind disturbance; and either can have a constant component, i.e., $\eta(s) = \eta_1/s + \ldots$. For the constant component to have no long term effect requires

$$d_{\eta_{ss}} = \lim_{s \to 0} s \left\{ \frac{\dot{N}_\eta^d + G_\theta^{\delta_e} \dot{N}_\eta^{d\,\theta}_{\delta_e}}{\Delta_{sys}} \right\} \eta(s) \qquad (28)$$

$$= \eta_1 \lim_{s \to 0} \{\ \} = 0$$

This will be zero when there is at least one net free s in the numerator.

Case 1: $\eta_1 = w_g$

$$d_{w_{g_{ss}}} = w_g \lim_{s \to 0} \left\{ \frac{\dot{D}_{w_g}^d + G_\theta^{\delta_e} \dot{B}_{w_g \delta_e}^{d\,\theta}}{G_d^{\delta_e} \dot{D}_{\delta_e}^d} \right\} \qquad (29)$$

Because the numerator is a constant as $s \to 0$, the free s needed to make the whole thing approach zero must come from the denominator. Consequently, a $K_d^{\delta_e}/s$ component is needed in the $G_d^{\delta_e}$ control path. A similar argument applies for trim changes resulting in Z_o and M_o lift and pitching accelerations applied to the vehicle. Also, note that any shear component to w_g will result in a steady-state error even with an integral controller.

Case 2: $\eta_1 = u_g$

$$d_{u_{g_{ss}}} = u_g \lim_{s \to 0} s \left\{ \frac{\dot{C}_{u_g}^d + G_\theta^{\delta_e} \dot{A}_{u_g \delta_e}^{d\,\theta}}{G_d^{\delta_e} \dot{D}_{\delta_e}^d} \right\} \qquad (30)$$

A free s occurs naturally in this numerator, so for $d_{u_{g_{ss}}}$ to be zero requires only that $\Delta_{sys}(0)$ be a constant or lower order in s. This means that $G_d^{\delta_e}(s)\big]_{s \to 0} \to K_{\delta_e}^d$ is satisfactory. However, head or tail winds invariably have a shear component, so a $K_d^{\delta_e}/s$ is desirable to help counter these.

These elementary considerations indicate that the most undesirable disturbance inputs are wind shears. In principle, the worst of these is a shear normal to the flight path, for this will cause a steady-state error in path. In practice, however, all shears occurring near the terminal condition give cause for concern because their effects are countered primarily by the integral control. This is inherently slow in action, as will be appreciated better with the aid of the concrete examples of the next section. The promise of zero steady-state error is, accordingly, more academic than real.

Additional "steady-state" requirements on regulation against disturbances can be derived if a shorter time scale is presumed. This can be done by considering the two-degree-of-freedom short-period characteristics instead of the complete three-degree-of-freedom equations. Any "final" values found using the short-period equations apply for time intervals which are large compared with the system's settling time, but not so long as to be comparable with phugoid periods. Thus the short-period approximation is valuable to treat some mid-frequency response properties.

Using the short-period approximation (see Table 2),

$$d_\eta = \left\{ \frac{Z_\eta \left[s^2 - (M_q + M_{\dot\alpha}) s - \left(M_\alpha - \frac{M_\eta}{Z_\eta} Z_\alpha \right) \right] + G_\theta^{\delta e} \left(M_{\delta_e} Z_\eta - Z'_{\delta_e} M_\eta \right)}{\Delta_{sys}} \right\} \eta \qquad (31)$$

This equation is most pertinent for a w-gust disturbance. When $\eta_1 = w_g$,

$$d_{w_{g_{ss}}} = w_g \lim_{s \to 0} \left\{ \frac{Z_w s \left[s - (M_q + M_{\dot\alpha}) \right] + G_\theta^{\delta e} (M_{\delta_e} Z_w - Z'_{\delta_e} M_w)}{\Delta_{sys}} \right\} \qquad (32)$$

$\Delta_{sys}(0)$ will be a constant if $K_d^{\delta e}$ is the lowest frequency feedback, or if the time span considered is relatively short, such that a $K_d^{\delta e}/s$ control will have little effect. Then, to obtain a net free s in the numerator, $G_\theta^{\delta e}$ must, itself, contain one. Thus we can establish a desire for pitching velocity rather than attitude feedback to improve the gust

TABLE 2

SHORT PERIOD EQUATIONS AND TRANSFER FUNCTIONS

Equations of Motion

$$[(1-Z_{\dot{h}}^{\cdot\cdot})s - Z_w]sd + Z_\alpha\theta = \overbrace{-Z_{\delta_e}\left(1-\frac{Z_{\delta_f}}{Z_{\delta_e}}G_c\right)}^{Z'_{\delta_e}}\delta_e - Z_{\delta_f}\delta_f - Z_\eta\eta$$

$$(M_{\dot{w}}s + M_w)sd + [s^2-(M_q+M_{\dot{\alpha}})s - M_\alpha]\theta = M_{\delta_e}\delta_e - M_\eta\eta$$

A $\delta_e \rightarrow \delta_f$ direct crossfeed and a possible $a_z \rightarrow \delta_f$ feedback to give the $Z_{\dot{h}}^{\cdot\cdot}$ are taken into account in these vehicle equations; and $M_{\delta_f} = 0$.

Characteristic Function

$$\Delta = (1-Z_{\dot{h}}^{\cdot\cdot})s^2\left\{s^2-\left(M_q+M_{\dot{\alpha}}+\frac{Z_w}{1-Z_{\dot{h}}^{\cdot\cdot}}\right)s-\left(M_\alpha-\frac{Z_wM_q}{1-Z_{\dot{h}}^{\cdot\cdot}}\right)\right\}$$

Numerator*

$$N_\delta^d = -Z_\delta\left[s^2-(M_q+M_{\dot{\alpha}})s-\left(M_\alpha-\frac{M_\delta}{Z_\delta}Z_\alpha\right)\right]$$

$$N_\eta^d = Z_\eta\left[s^2-(M_q+M_{\dot{\alpha}})s-\left(M_\alpha-\frac{M_\eta}{Z_\eta}Z_\alpha\right)\right]$$

$$N_\delta^\theta = s\left\{[M_\delta(1-Z_{\dot{h}}^{\cdot\cdot})+Z_\delta M_{\dot{w}}]s-(M_\delta Z_w - Z_\delta M_w)\right\}$$

$$N_\eta^\theta = -s\left\{[M_\eta(1-Z_{\dot{h}}^{\cdot\cdot})+Z_\eta M_{\dot{w}}]s-(M_\eta Z_w - Z_\eta M_w)\right\}$$

Coupling Numerators

$$N_{\delta_e\delta_f}^{\theta\ d} = -Z_{\delta_f}M_{\delta_e}$$

$$N_{\eta\ \delta_e}^{d\ \theta} = M_{\delta_e}Z_\eta - Z'_{\delta_e}M_\eta$$

Modal Response Ratio

$$\left[\frac{U_o\theta}{\dot{d}}\right]_{s_i} = \left[\frac{(1-Z_{\dot{h}}^{\cdot\cdot})}{-Z_w}\left(s-\frac{Z_w}{1-Z_{\dot{h}}^{\cdot\cdot}}\right)+G_d^{\delta_f}\frac{Z_{\dot{\delta}_f}}{Z_w}\right]_{s_i}$$

*For these short-period equations it is possible to define N_δ^d without having to resort to numerators that are ratios of polynomials.

regulation at mid-frequencies. This permits the drift from the beam caused by a normal gust to be reduced by virtue of the aircraft's weather-cocking tendency. This would not be possible if the aircraft rigidly maintained its pitch attitude.

Implied Requirement on δ_f

The direct lift control, be it spoiler or flap, can have only a very limited control power compared with the elevator-wing combination. Consequently the longer time (near steady-state) control should be elevator to avoid saturating the DLC. The time scale of interest here is relatively short, so the short-period equations (Table 2) can again be used to define a kind of "short time steady-state." For a trim change defined by an incremental lift, Z_o, and pitching, M_o, accelerations, the flap deflection will be,

$$\begin{aligned}\delta_f &= -G_d^{\delta_f}\, d \\ &= G_d^{\delta_f}\frac{\left\{-\left[s^2-(M_q+M_{\dot\alpha})s-M_\alpha\right]-G_\theta^{\delta_e}M_{\delta_e}\right\}Z_o+(-Z_\alpha+G_\theta^{\delta_e}Z'_{\delta_e})M_o}{\Delta_{sys}}\end{aligned} \tag{33}$$

If $G_\theta^{\delta_e}$ is presumed to have a free s, and Z_o and M_o have constant terms, e.g., $Z_o(s) = Z_1/s + \ldots$, then (using Eq. 33 and the short-period version of Eq. 19)

$$\delta_{f_{ss}} = \lim_{s\to 0}\left\{\frac{G_d^{\delta_f}(M_\alpha Z_1 - Z_\alpha M_1)}{G_d^{\delta_e}N_{\delta_e}^d + G_d^{\delta_f}N_{\delta_f}^d}\right\} \tag{34}$$

For $\delta_{f_{ss}}$ to be zero then requires $G_d^{\delta_f}$ to be one order higher in s than $G_d^{\delta_e}$.

From the above steady-state (long time as well as short time) considerations we have shown that the minimum forms of the feedbacks needed to satisfy reasonable steady-state guidance, control, and regulation requirements are:

$$G_{\dot{d}}^{\delta e} = \frac{K_{\dot{d}}^{\delta e}}{s} + K_{\dot{d}}^{\delta e} \tag{35}$$

$$G_{\theta}^{\delta e} = K_{\theta} s \tag{36}$$

and, if DLC is used,

$$G_{\dot{d}}^{\delta f} = K_{\dot{d}}^{\delta f} \text{ or higher terms in } s \tag{37}$$

Having disposed of the feedback requirements imposed by steady-state considerations, we shall now turn to a short discussion of the higher frequency feedbacks. The simplest of these is the attitude transfer function, $G_{\theta}^{\delta e}$. When the short term attitude regulation requirement is considered — implying attitude stiffening at short-period frequencies to provide a craft that is stable and solid in attitude — the $G_{\theta}^{\delta e}$ of Eq. 36 is modified to a simple washout. This retains the free s in the numerator of $G_{\theta}^{\delta e}$, with its favorable consequences in regulating against wind disturbances, while still providing an attitude feedback at short period frequencies. The washout time constant $1/T_w$ must, of course, be such that $1/T_w$ is less than ω_{sp}. Further, taking higher frequency effects into account, a pitch rate feedback $K_{\dot{\theta}} s$ would be desirable to provide greater short-period attitude damping and attitude loop bandwidth. This would then permit improved altitude loop gain margins and, thereby, a greater altitude bandwidth. Consequently the desired general form for the pitch attitude feedback is

$$G_{\theta}^{\delta e} = \frac{K_{\theta} s}{s + (1/T_w)} + K_{\dot{\theta}} s \tag{38}$$

The remaining requirements for the general form of the feedback controller dynamics can be derived by analogy with the lateral case. Thus, with the attitude feedback washed out at low frequencies, $K_{\dot{d}}$ feedbacks are needed to improve the path damping. As is evident from Table 3, which shows the closed-loop characteristic function coefficients, this can be a useful feedback to both elevator and DLC. In fact, because the high frequency limiting factors on DLC and elevator closures can be somewhat different, a system using the d feedbacks to both controls is desirable. Recall, however, the implied requirement that $G_d^{\delta f}$ be one order of s higher than $G_d^{\delta e}$. Thus, appropriate general forms for the path deviation feedbacks are

$$G_d^{\delta e} = \frac{K_{\bar{d}}^{\delta e}}{s} + K_d^{\delta e} + K_{\dot{d}}^{\delta e}\, s \tag{39}$$

$$G_d^{\delta f} = K_d^{\delta f} + K_{\dot{d}}^{\delta f}\, s \tag{40}$$

Without going further into all the ramifications and justifications behind these selections, a general summary of the feedbacks, their purposes, and qualitative requirements is provided in Table 4.

TABLE 3

CLOSED-LOOP CHARACTERISTIC FUNCTION COEFFICIENTS
USING SHORT-PERIOD AIRCRAFT EQUATIONS

$$s^5: \quad (1 - Z_{\ddot{h}})$$

$$s^4: \quad \frac{1}{T_w}(1-Z_{\ddot{h}}) - (1-Z_{\ddot{h}})\left(M_q + M_{\dot{\alpha}} + \frac{Z_w}{1-Z_{\ddot{h}}}\right) + K_{\dot{\theta}}[M_{\delta_e}(1-Z_{\ddot{h}}) + Z'_{\delta_e}M_w] - [Z'_{\delta_e}K_{\dot{d}}^{\delta_e} + Z_{\delta_f}K_{\dot{d}}^{\delta_f}]$$

$$s^3: \quad (1-Z_{\ddot{h}})\left[-\left(M_\alpha - \frac{Z_w M_q}{1-Z_{\ddot{h}}}\right) - \frac{1}{T_w}\left(M_q + M_{\dot{\alpha}} + \frac{Z_w}{1-Z_{\ddot{h}}}\right) + \left(K_\theta + \frac{K_{\dot{\theta}}}{T_w}\right)\left(M_{\delta_e} + \frac{Z'_{\delta_e}M_w}{1-Z_{\ddot{h}}}\right) - K_{\dot{\theta}}\frac{(M_{\delta_e}Z_w - Z_{\delta_e}M_w)}{1-Z_{\ddot{h}}}\right]$$
$$- Z'_{\delta_e}\left[K_d^{\delta_e} + \left(\frac{1}{T_w} - M_q - M_{\dot{\alpha}}\right)K_{\dot{d}}^{\delta_e}\right] - Z_{\delta_f}\left[K_d^{\delta_f} + \left(\frac{1}{T_w} - M_q - M_{\dot{\alpha}}\right)K_{\dot{d}}^{\delta_f}\right] - Z_{\delta_f}M_{\delta_e}K_{\dot{d}}^{\delta_f}K_{\dot{\theta}}$$

$$s^2: \quad (1-Z_{\ddot{h}})\left\{\left\{-\frac{1}{T_w}\left(M_\alpha - \frac{Z_w M_q}{1-Z_{\ddot{h}}}\right) - \left(K_\theta + \frac{K_{\dot{\theta}}}{T_w}\right)\frac{M_{\delta_e}Z_w - Z'_{\delta_e}M_w}{1-Z_{\ddot{h}}} - \frac{Z'_{\delta_e}}{1-Z_{\ddot{h}}}\left\{K_d^{\delta_e} + K_d^{\delta_e}\left(\frac{1}{T_w} - M_q - M_{\dot{\alpha}}\right) - K_{\dot{d}}^{\delta_e}\left[\frac{1}{T_w}(M_q + M_{\dot{\alpha}}) + \left(M_\alpha - \frac{M_{\delta_e}}{Z'_{\delta_e}}Z_\alpha\right)\right]\right\}\right\}\right.$$
$$\left. - \frac{Z_{\delta_f}}{1-Z_{\ddot{h}}}\left\{K_d^{\delta_f}\left(\frac{1}{T_w} - M_q - M_{\dot{\alpha}}\right) - K_{\dot{d}}^{\delta_f}\left[\frac{1}{T_w}(M_q + M_{\dot{\alpha}}) + \left(M_\alpha - \frac{M_{\delta_f}}{Z_{\delta_f}}Z_\alpha\right)\right]\right\} - \frac{Z_{\delta_f}M_{\delta_e}}{1-Z_{\ddot{h}}}\left[K_{\dot{d}}^{\delta_f}\left(K_\theta + \frac{K_{\dot{\theta}}}{T_w}\right) + K_d^{\delta_f}K_{\dot{\theta}}\right]\right\}\right\}$$

$$s^1: \quad -Z'_{\delta_e}\left\{K_{\dot{d}}^{\delta_e}\left(\frac{1}{T_w} - M_q - M_{\dot{\alpha}}\right) - K_d^{\delta_e}\left[\frac{1}{T_w}(M_q + M_{\dot{\alpha}}) + \left(M_\alpha - \frac{M_{\delta_e}}{Z'_{\delta_e}}Z_\alpha\right)\right] - K_{\dot{d}}^{\delta_e}\frac{1}{T_w}\left(M_\alpha - \frac{M_{\delta_e}}{Z'_{\delta_e}}Z_\alpha\right)\right\}$$
$$+ Z_{\delta_f}\left\{K_d^{\delta_f}\left[\frac{1}{T_w}(M_q + M_{\dot{\alpha}}) + \left(M_\alpha - \frac{M_{\delta_f}}{Z_{\delta_f}}Z_\alpha\right) - M_{\delta_e}\left(K_\theta + \frac{K_{\dot{\theta}}}{T_w}\right)\right] + K_{\dot{d}}^{\delta_f}\frac{1}{T_w}\left(M_\alpha - \frac{M_{\delta_f}}{Z_{\delta_f}}Z_\alpha\right)\right\}$$

$$s^0: \quad Z'_{\delta_e}\left\{K_{\dot{d}}^{\delta_e}\left[\frac{1}{T_w}(M_q + M_{\dot{\alpha}}) + \left(M_\alpha - \frac{M_{\delta_e}}{Z_{\delta_e}}Z_\alpha\right)\right] + K_d^{\delta_e}\frac{1}{T_w}\left(M_\alpha - \frac{M_{\delta_e}}{Z'_{\delta_e}}Z_\alpha\right)\right\} + Z_{\delta_f}\left\{K_d^{\delta_f}\frac{1}{T_w}\left(M_\alpha - \frac{M_{\delta_f}}{Z_{\delta_f}}Z_\alpha\right)\right\}$$

$$s^{-1}: \quad Z'_{\delta_e}K_{\dot{d}}^{\delta_e}\frac{1}{T_w}\left(M_\alpha - \frac{M_{\delta_e}}{Z_{\delta_e}}Z_\alpha\right)$$

TABLE 4

LONGITUDINAL FEEDBACKS — PURPOSES AND QUALITATIVE REQUIREMENTS

FEEDBACK TERMS	FUNCTION	REQUIREMENT	REMARKS
K_θ	Short-Period Attitude Stiffness	$\theta \rightarrow \delta_e$ in short-period frequency range $(1/T_w < \omega_{sp})$	Windproofing and attitude stiffening conflict
$K_{\dot{\theta}}$	Short-Period Damping; Path Loop Bandwidth Extension Capability	$\dot{\theta} \rightarrow \delta_e$ in short-period frequency range	
T_w	Short Term w_g Windproofing	$s[s-(M_q+M_{\dot{\alpha}})] + G_\theta^{\delta_e} M_{\delta_e}$ small over w_g frequencies	
K_d	Path Acquisition and Stiffness Windproofing (u_g step, w_g pulse)	K_d sets dominant path mode frequency; made as large as possible consistent with stability and limiting	Altitude control bandwidth with $d,\theta \rightarrow \delta_e$ is limited by $1/T_{\theta 2}$; can be increased significantly by $d,\dot{d}$, or $\dot{h} \rightarrow \delta_f$. Therefore δ_f can be big help in approach and flare precision.
$K_{\bar{d}}$	Higher-Order Path Following Trim Windproofing (w_g step)	$K_d/K_{\bar{d}}$ sets trim response time	$K_{\bar{d}}^{\delta_f} = 0$ for δ_e to handle trim
$K_{\dot{d}}$ or $K_{\dot{h}}$	Path Damping	Sets path mode damping ratio $0.64 < \zeta_{\text{path mode}} < 1$	$\dot{d}$ suffers from beam noise; $\dot{h}$ requires trim bias to offset steady-state sink rate.
K_θ		$\theta \rightarrow \delta_e$ in long-period frequency range	Conflicts with windproofing.

SECTION III

DEVELOPMENT AND ANALYSIS OF EXAMPLE SYSTEMS

To provide concrete examples of approach systems, three longitudinal approach controllers shall be developed in this section. (The results are used in Ref. 1 to compute average performance measures and probabilities of approach success.) The three systems developed can be considered as competitors throughout the analysis; that is, they can be considered in terms of: dynamic characteristics, performance measures and probability of approach success.

The aircraft to be controlled will be a DC-8 defined by the landing approach configuration parameters given in Table 5. The aircraft transfer

TABLE 5

DC-8 PARAMETERS FOR LANDING APPROACH CONFIGURATION

GEOMETRY AND INERTIAL PROPERTIES			LONGITUDINAL STABILITY AXES			LATERAL BODY AXES		
h	(ft)	0	X_u	(1/sec)	−0.0373	Y_v	(1/sec)	−0.0887
M	(−)	.204	X_w	(1/sec)	0.136	$Y_{\delta_a}^*$	(1/sec)	0
V_{T_o}	(ft/sec)	228.	X_{δ_e}	(ft/sec^2/rad)	0	$Y_{\delta_r}^*$	(1/sec)	0.031
γ_o	(deg)	−2.8°	X_{δ_T}	(ft/sec^2/%)	0.106	L_β	(1/sec^2)	−1.40
q	(lb/ft^2)	61.8	Z_u	(1/sec)	−0.283	L_p	(1/sec)	−1.04
S	(ft^2)	2758.	Z_w	(1/sec)	−0.750	L_r	(1/sec)	0.474
b	(ft)	142.4	$Z_{\dot{w}}$	(−)	0	L_{δ_a}	(1/sec^2)	1.13
c	(ft)	22.16	Z_{δ_e}	(ft/sec^2/rad)	−9.25	L_{δ_r}	(1/sec^2)	0.159
W	(lb)	180,000.	Z_{δ_T}	(ft/sec^2/%)	−0.00097	N_β	(1/sec^2)	0.368
m	(slugs)	5,580.	M_u	(1/sec-ft)	0	N_p	(1/sec)	−0.029
I_x	(slug-ft^2)	3.2×10^6	M_w	(1/sec-ft)	−0.00461	N_r	(1/sec)	−0.257
I_y	(slug-ft^2)	3.8×10^6	$M_{\dot{w}}$	(1/ft)	−0.00085	N_{δ_a}	(1/sec^2)	0
I_z	(slug-ft^2)	6.6×10^6	M_q	(1/sec)	−0.594	N_{δ_r}	(1/sec^2)	−0.368
I_{xz}	(slug-ft^2)	0	M_{δ_e}	(1/sec^2)	−0.923			
X_{CG}	(% c)	25.2	M_{δ_T}	(1/sec^2/%)	0.000623			
δ_{F_o}	(deg)	50	M_α	(1/sec^2)	−1.05			
α_o	(deg)	0.62	$M_{\dot{\alpha}}$	(1/sec)	−0.1936			

function characteristics for control inputs are shown in the Bode plots of Fig. 7. The notation in the numerical transfer functions shown on these plots is a shorthand in which (1/T) represents a first-order term with time constant T, and [ζ, ω_n] represents a second-order factor with damping ratio ζ and undamped natural frequency ω_n. For example, in Fig. 7, $1/T_{\theta_1} = 0.101$, $1/T_{\theta 2} = 0.646$, $\zeta_{sp} = 0.626$ and $\omega_{sp} = 1.231$. The same notation is used in the complete compilation of transfer functions and coupling numerators given in Table 6.

The control equations and functions accomplished by the three systems are given in Table 7. The systems are arranged from "A" to "C" in order of decreasing complexity and capability with "A" also standing for "advanced" and "C" for "conventional." All of the systems can acquire and maintain position on a straight line glide slope beam with well-damped path mode responses. However, System C is not suitable for following higher order paths with zero steady state error. The major distinction between Systems B and C is in the θ feedback, which is washed out at very low frequencies on System B and not at all on System C. The washout is intended to improve the w_g windproofing, the steady-state following of higher order paths, and to remove the effects of any steady-state θ biases. This is achieved at the expense of a slight amount of path damping and bandwidth. Consequently, the superiority of System B in w_g windproofing and steady-state operations may be offset, for other inputs, by its smaller bandwidth.

System A is representative of the elevator axis of an advanced controller, typical of the forthcoming generation of low level approach and automatic landing systems. Appropriate feedbacks exist for all the functions listed for longitudinal control in Table 7.

All of the example systems can be improved by the addition of an airspeed control. However, as will become evident later, the airspeed control properties of the three systems as they stand are nearly identical. Further, this similarity will not be changed if the same airspeed controller is added to all systems. Consequently, for the sake of simplicity, we have not provided airspeed control loops.

The control equations for the three systems are given in the last row of Table 7 in terms of δ_{e_c}. This is the commanded elevator which must

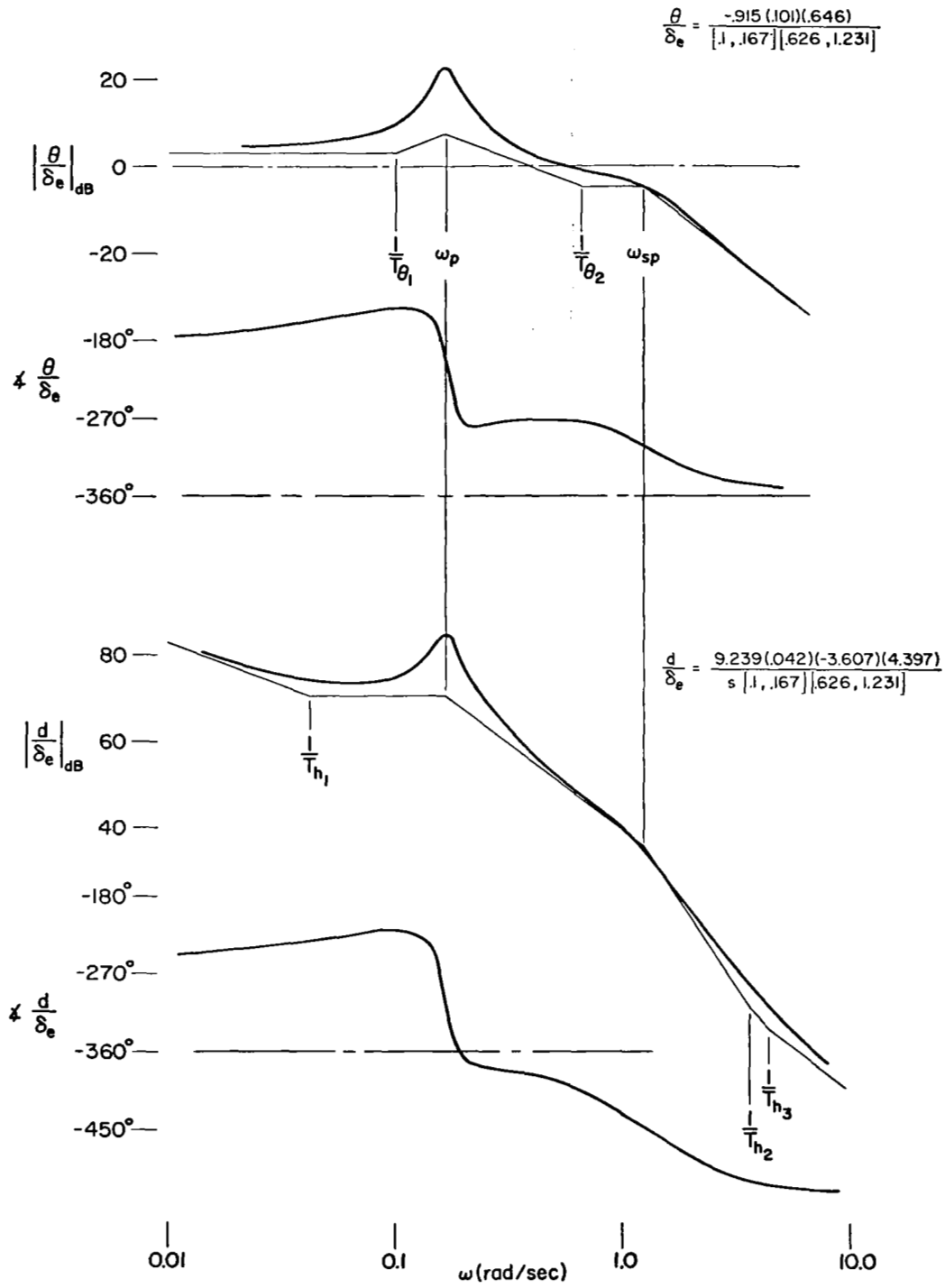

Figure 7. Bode Plots of Elevator Transfer Functions for the Bare Airframe

TABLE 6

LONGITUDINAL TRANSFER FUNCTIONS FOR THE DC-8 IN LANDING APPROACH CONFIGURATION

Denominator

$$\Delta = [0.10 , 0.167][0.626 , 1.231]$$

Numerators

δ_e Control Input

$$N^{u}_{\delta_e} = -1.258(4.03)(-4.082)$$

$$N^{w}_{\delta_e} = -9.25(23.34)[0.107 , 0.198]$$

$$N^{\theta}_{\delta_e} = -0.9151(0.101)(0.646)$$

$$N^{\dot{h}}_{\delta_e} = 9.239(0.042)(-3.607)(4.397)$$

$$N^{\dot{d}}_{\delta_e} = 9.25(0.035)(-3.606)(4.396)$$

u_g Gust Input

$$N^{u}_{u_g} = 0.0373(1.543)[0.599 , 0.857]$$

$$N^{w}_{u_g} = 0.283(0)(0)(0.594)$$

$$N^{\theta}_{u_g} = -0.0002406(0)(5.424)$$

$$N^{\dot{h}}_{u_g} = -0.2845(0.007)[0.386 , 1.027]$$

$$N^{\dot{d}}_{u_g} = -0.283(0)[0.384 , 1.025]$$

w_g Gust Input

$$N^{u}_{w_g} = -0.1360(0)[0.486 , 0.795]$$

$$N^{w}_{w_g} = 0.3498(4.379)[0.118 , 0.166]$$

$$N^{\theta}_{w_g} = -0.001755(0)(-1.475)(-0.000464)$$

$$N^{\dot{h}}_{w_g} = -0.7425(1.243)[0.081 , 0.214]$$

$$N^{\dot{d}}_{w_g} = -0.75(1.234)[0.091 , 0.214]$$

Coupling Numerators

$$N^{\theta\, u}_{\delta_e u_g} = -0.03413(1.751)$$

$$N^{\theta\, w}_{\delta_e u_g} = -0.2612(0)$$

$$N^{u\, w}_{\delta_e u_g} = 0.345(1.102)(22.243)$$

$$N^{\theta\, u}_{\delta_e w_g} = 0.1223(0)$$

$$N^{\theta\, w}_{\delta_e w_g} = -0.01624(0.092)(39.955)$$

$$N^{u\, w}_{\delta_e w_g} = -1.258(-0.696)(23.626)$$

TABLE 7

CONTROL EQUATIONS AND FUNCTIONS PERFORMED BY THE EXAMPLE AUTOMATIC LONGITUDINAL SYSTEMS

	FUNCTION	SYSTEM		
		A	B	C
Attitude Control and Regulation	Short-Period Attitude Stiffness	$\theta \rightarrow \delta_e$ in short-period frequency range		
	Short-Period Damping; Path Loop Bandwidth Extension Capability	$\dot{\theta} \rightarrow \delta_e$ in short-period frequency range		
	Short Term w_g Windproofing	High-frequency θ washout	Low-frequency θ washout	No θ washout
Path Control and Regulation	Higher-order Path Following Trim Windproofing (w_g step)	$\int d\ dt \rightarrow \delta_e$	Low-frequency θ washout	
	Path Acquisition and Stiffness Windproofing (u_g step, w_g pulse)	$d \rightarrow \delta_e$		
	Path Damping	$\dot{h} \rightarrow \delta_e$	$\theta \rightarrow \delta_e$ in long-period frequency range	$\theta \rightarrow \delta_e$
Control Equations		$-\delta e_c = \frac{K_{\bar{d}} + K_d s}{s(T_f s + 1)} d_\epsilon + K_{\dot{h}} \dot{h} + \frac{K_\theta s}{s + 1/T_{wo}} \theta + K_{\dot{\theta}} \dot{\theta}$	$-\delta e_c = \frac{K_d d_\epsilon}{T_f s + 1} + \frac{K_\theta s}{s + 1/T_{wo}} \theta$	$-\delta e_c = \frac{K_d d_\epsilon}{T_f s + 1} + K_\theta \theta$

be converted to actual elevator deflection by the flight control and surface actuation systems. The actuator characteristics (Y_a) will be approximated here by a first-order lag with $1/T_a$ equal to 15 sec^{-1}. Although grossly oversimplified, this is an adequate approximation to the actuator properties for the low frequency range of primary interest.

Block diagrams corresponding to the control equations are given in Figs. 8 and 9 for Systems A and C. A block diagram for System B would be essentially the same as that in Fig. 9, with the replacement of the attitude feedback, K_θ, by the transfer function, $K_\theta T_{wo} s/(T_{wo} s + 1)$.

Having defined the systems qualitatively, we shall now turn to the quantitative descriptions which will be developed for each system. First, the closed-loop dynamic characteristics will be considered in terms of $j\omega$ Bode and Bode root locus plots for the systems as adjusted. Then, typical time histories of the systems will be discussed for command and disturbance inputs.

Conventional System (System C)

The analysis of System C will be described in two steps: the closing of an attitude inner loop followed by the closing of a path deviation outer loop. The connections and interplay between these two operations is central to the synthesis procedure, because the attitude loop provides the equalization necessary for the path deviation loop to be closed such that rapid, stable, well-damped responses result. Consequently, we will take some pains to point out these connections in a discussion of the analysis.

A $j\omega$-Bode plot for the open-loop attitude to elevator transfer function and a closed-loop Bode root-locus for the same system are shown in Fig. 10. The Bode root-locus comprises both real and complex roots, the real roots being shown with the heavy line (so-called siggy Bode plots), whereas the complex roots are dotted. (The values of real roots and closed-loop undamped natural frequencies are read using the abscissa, while the closed-loop damping ratios are parameters along the complex branches. Gain, of course, is the ordinate.) The Bode root-locus shows that as the gain, K_θ, is increased, the damping ratio and total damping of the phugoid mode are also increased, resulting (at high gain) in two real roots which approach

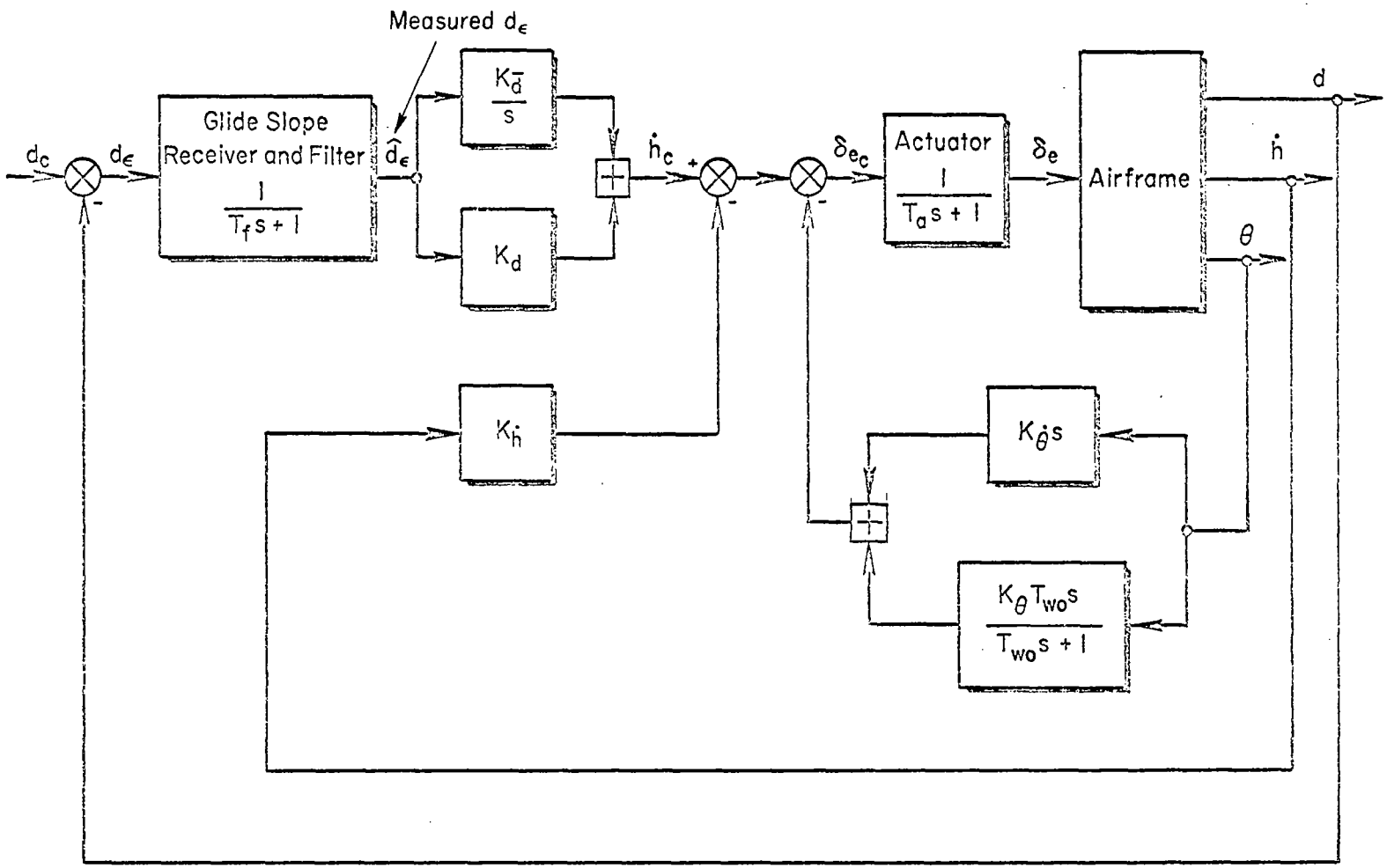

Figure 8. Block Diagram of Advanced System [A]

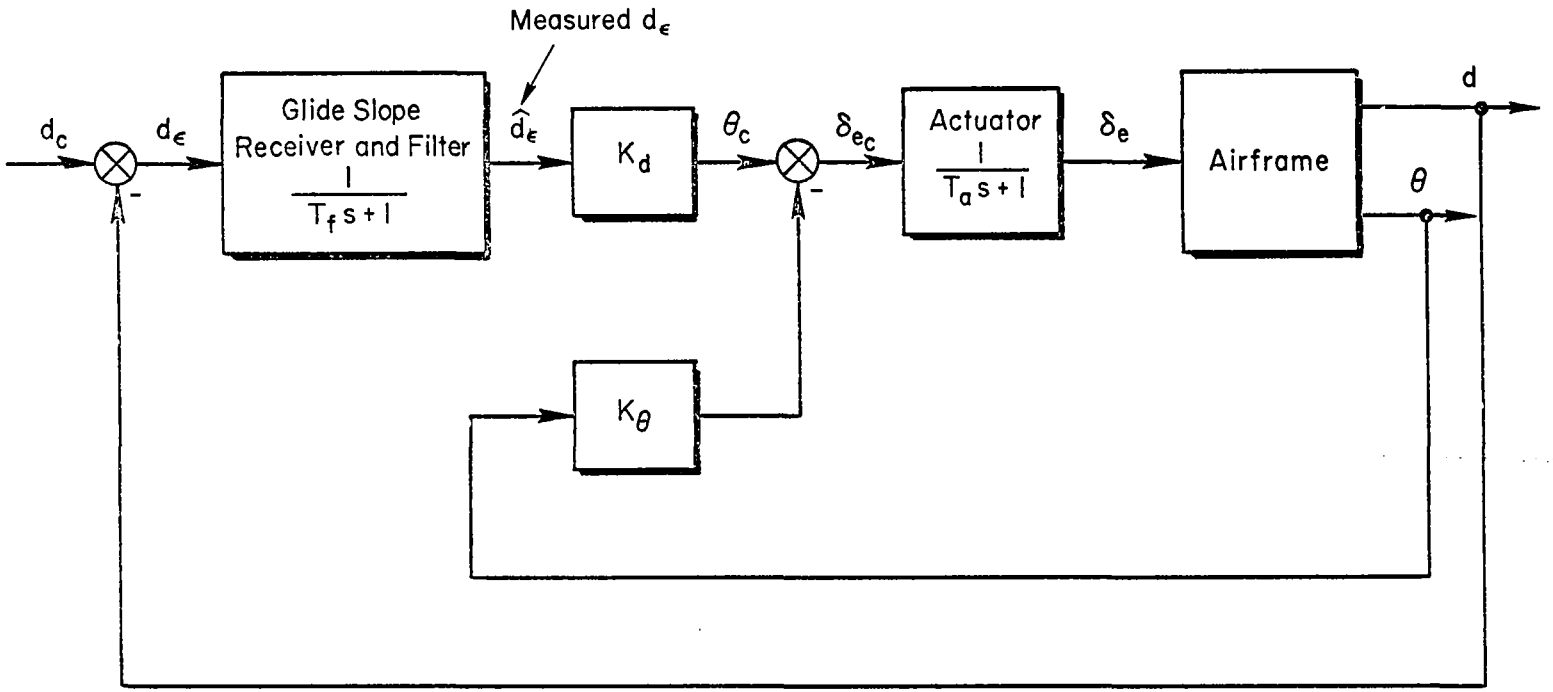

Figure 9. Block Diagram of Conventional System [C]

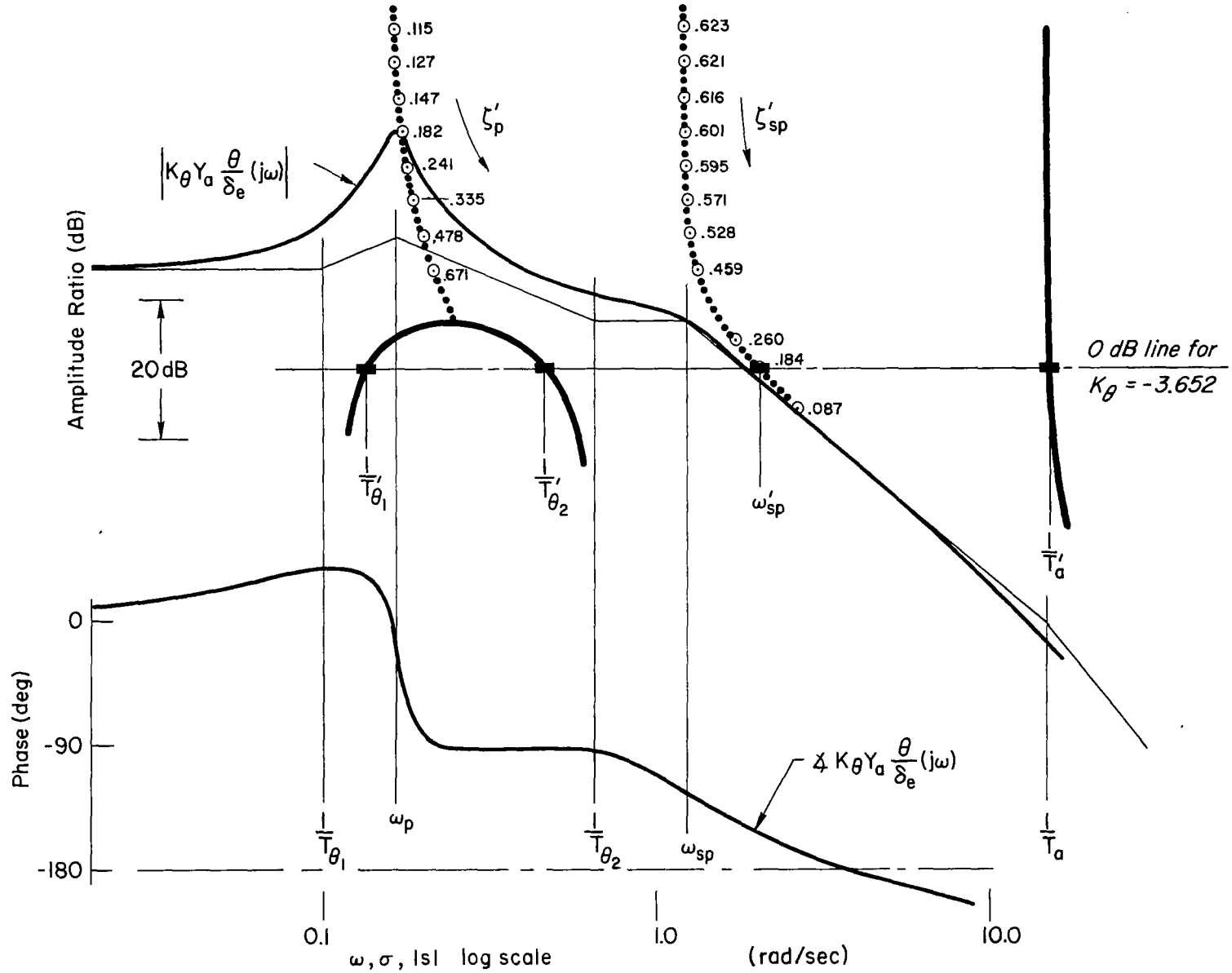

Figure 10. System Survey for Attitude Loop Closure for System C

the zeros, $-1/T_{\theta_1}$ and $-1/T_{\theta_2}$. For the same gain variation, the closed-loop short-period damping and damping ratio are decreased. Thus, the increased phugoid damping is obtained at the expense of the short-period damping. For relatively low gain, the decrease in short-period damping is reflected primarily in the short-period damping ratio because the short-period undamped natural frequency is essentially unchanged. At moderate and high gains, the short-period natural frequency increases, resulting in an even faster decrease of short-period damping ratio with gain. Finally, the closed-loop actuator characteristics are but slightly modified from the open-loop properties for reasonable values of gain. For the nominal zero dB line shown (K_θ is -3.65) the phugoid roots are shown as $1/T'_{\theta_1}$ and $1/T'_{\theta_2}$ (the prime indicating one loop has been closed and the T_{θ_1} and T_{θ_2} indicating the zeros being approached), and the closed-loop short-period damping ratio is 0.184. With this closure, there is a wide spread between $1/T'_{\theta_1}$ and $1/T'_{\theta_2}$, yet the short-period damping ratio is still moderate ($\zeta'_{sp} = 0.184$ gives 0.61 cycles to half amplitude).

Only the poles of the glide slope deviation to elevator transfer function are modified by the closure of the θ to δ_e loop; the numerator is still that of the airframe alone. The deviation to deviation-error open-loop transfer function, with the attitude loop closed, is shown in the system survey in Fig. 11, where the $j\omega$-Bode reflects the open-loop zeros of the numerator, $N^{\dot{d}}_{\delta_e}(s)$, the closed-loop poles resulting from the attitude closure, and a beam noise smoothing filter (Y_f) with a time constant of 0.5 sec. The Bode root-locus of this (outer) loop is also provided in the figure. Here it is seen that the very-low-frequency mode stemming from the free s advances toward $1/T_{h_1}$ as gain increases, while the two phugoid roots rendezvous and become a new second order; the short-period damping ratio increases somewhat, and the short-period undamped natural frequency remains essentially unchanged.

The crossover region (frequency region near the intersection of the 0 dB line and the $j\omega$ Bode) compatible with good closed-loop response lies along the approximately -20 dB per decade slope starting at about $1/T'_{\theta_1}$. Selecting a gain for this beam deviation loop involves a compromise between the dominant path mode (the phugoid) and the mode associated with the very

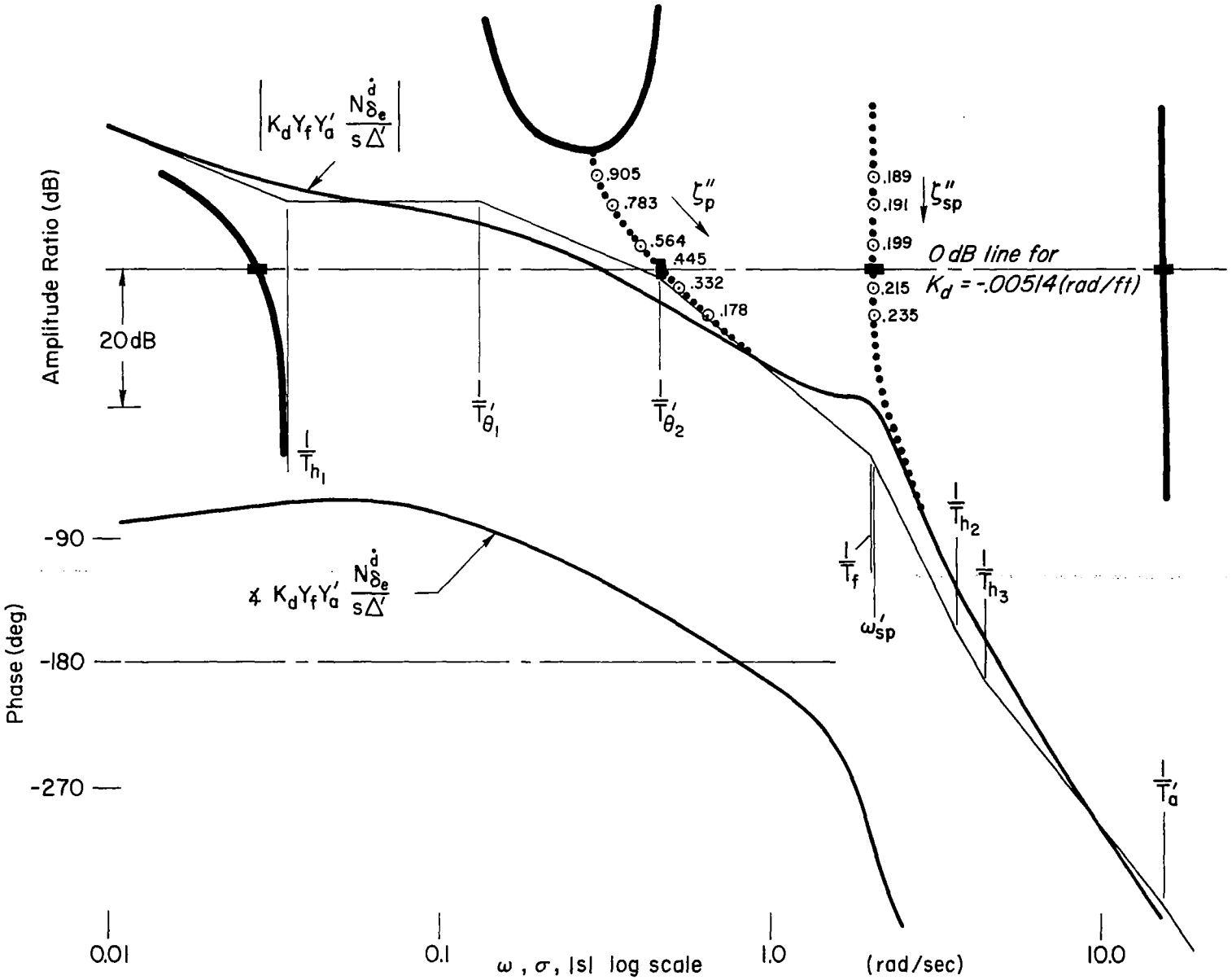

Figure 11. System Survey for Beam Deviation Loop Closure for System C

low frequency dipole pair. The higher the gain the less the effect of the dipole, yet the less well damped becomes the quadratic path mode. The gain selected is therefore made to compromise these factors. The gain value, K_d, chosen results in a crossover frequency somewhat greater than 0.2 rad/sec. The dominant mode with this gain is the path control quadratic (nee phugoid) with $\zeta_p'' = 0.445$ and $\omega_p'' = 0.465$ rad/sec. The very-low-frequency root at 0.028 will be dominant in some degree of freedom, such as speed, although in the deviation response to a d command its effect will be partially removed by the lead at $1/T_{h_1} = 0.035$. Thus we have achieved a system which exhibits a well damped, fairly rapid response path mode which is slightly contaminated by a very long time constant mode, together with a relatively high frequency, reasonably damped, short-period mode.

Let us now consider imaginary modifications to these nominal plots. In the deviation loop closure, the range of permissible crossovers would be extended if the breakpoints at $1/T'_{\theta_1}$ and $1/T'_{\theta_2}$ could be further separated. Also the siggy segments of the Bode root-locus would then be moved down relative to the asymptotic plot, such that the attainable path mode damping ratio for a given gain, K_d, would be increased. Unfortunately, with the feedbacks available in System C the maximum separation attainable is limited by $1/T_{\theta_1}$ and $1/T_{\theta_2}$, and these can be approached in the attitude loop closure only at the expense of an underdamped short-period. However, this short-period deficiency which is developed in the inner-loop closure is partially made up in the outer-loop closure, where ζ''_{sp} is slightly increased over ζ'_{sp}. If the airplane-alone had greater short-period damping, then a larger attitude loop gain could be used, thereby permitting an increased deviation loop bandwidth with the same damping ratio. Via this reasoning, a pitch rate damper would be useful even when the short-period damping ratio is large, as on this DC-8 example.

When only the attitude and deviation are permitted as feedbacks, the gains given here are nearly optimum, in that the resulting responses are rapid and well damped and the change in these responses will be relatively insensitive to changes in many of the vehicle parameters. From the sensitivity viewpoint, the primary effects are those of $1/T_{h_1}$, which will modify

the very-low-frequency closed-loop root; $1/T_{\theta_2}$ which profoundly affects the dominant quadratic path mode; and the short-period undamped natural frequency (ω_{sp}) and damping ratio (ζ_{sp}). The sensitivity of the closed-loop roots to other open-loop characteristics is not large. This is most easily appreciated by recognizing that the first-order sensitivities (Ref. 2), relating incremental changes in closed-loop roots to incremental changes in open-loop gain or open-loop roots, are inversely proportional to the slopes on the Bode root-locus. As can be seen from Figs. 10 and 11, these slopes are quite large at the chosen gains.

The closed-loop transfer functions for System C are given in Table 8. These data are used in Ref. 1 to compute the rms deviations due to u_g and w_g inputs.

TABLE 8

CLOSED-LOOP TRANSFER FUNCTIONS FOR SYSTEM C

$$\frac{\hat{d}_\epsilon}{u_g} = \frac{+0.566(0)(15.229)[0.134\ ,\ 2.087]}{(0.028)(2.066)(15.228)[0.445\ ,\ 0.465][0.206\ ,\ 2.039]}$$

$$\frac{\hat{d}_\epsilon}{w_g} = \frac{+1.5(0.111)(15.139)[0.291\ ,\ 1.76]}{(0.028)(2.066)(15.228)[0.445\ ,\ 0.465][0.206\ ,\ 2.039]}$$

$$\frac{\hat{d}_\epsilon}{d_{command}} = \frac{+2.0(0)(0.13)(0.46)(15.228)[0.18\ ,\ 2.05]}{(0.028)(2.066)(15.228)[0.445\ ,\ 0.465][0.206\ ,\ 2.039]}$$

$$\frac{u}{u_g} = \frac{0.0373(0.12)(1.35)(2.169)(15.228)[0.176\ ,\ 1.995]}{(0.028)(2.066)(15.228)[0.445\ ,\ 0.465][0.206\ ,\ 2.039]}$$

$$\frac{u}{w_g} = \frac{-0.136(2.051)(15.224)[-0.17\ ,\ 0.442][0.165\ ,\ 1.96]}{(0.028)(2.066)(15.228)[0.445\ ,\ 0.465][0.206\ ,\ 2.039]}$$

$$\frac{u}{d_{command}} = \frac{0.194(0)(4.03)(-4.082)}{(0.028)(2.066)(15.228)[0.445\ ,\ 0.465][0.206\ ,\ 2.039]}$$

Typical transient responses for a deviation command, d_c, and step u_g and w_g gust inputs are shown in Figs. 12 through 14. The step response to a d command is, as anticipated, dominated by the very-low-frequency dipole pair and the dominant path mode. Only a slight overshoot is present with the gains selected and this response is, in general, entirely satisfactory. The short-period properties show up primarily in the elevator trace. The attitude primarily simulates the altitude rate, as can be seen by comparing the $\dot{h}$ and θ traces. Finally, a small speed deviation occurs with a time constant given by the closed-loop mode, $1/T'_{h_1}$, which approaches $1/T_{h_1}$. This is more graphically demonstrated on the speed responses to u_g and w_g step disturbances.

System with Low Frequency Attitude Washout (System B)

System B is very similar to System C. The difference lies in the attitude feedback at very low frequencies which is washed out rather than a pure gain. This has several effects. Statically, the need to fly with a slight deviation to offset any steady-state attitude is removed. Dynamically, the following of beam deviation commands and response to w gusts can be made somewhat better.

The open- and closed-loop attitude dynamics are shown on Fig. 15. When this is compared with Fig. 10, the high frequency characteristics are seen to be very similar, whereas the very-low-frequency properties are quite different. The open-loop dc gain is zero, and the presence of the washout gives rise to a root at $-1/T'_{w_0}$. For the same gain as used on the conventional system, the short-period frequency is essentially the same, the damping ratio is very slightly larger, and the phugoid roots are in closer proximity to $1/T_{\theta_1}$ and $1/T_{\theta_2}$. All of these features have favorable effects in the outer loop.

The path deviation loop characteristics, with the attitude inner loop closed, are given in Fig. 16. By comparison with the conventional system, the low-frequency properties are close to those of a K/s system over a very wide frequency band. Consequently, the system gain can be set at almost any value in this range and result in a well-shaped response to a d_c command. The time scale of the response is, of course, scaled by

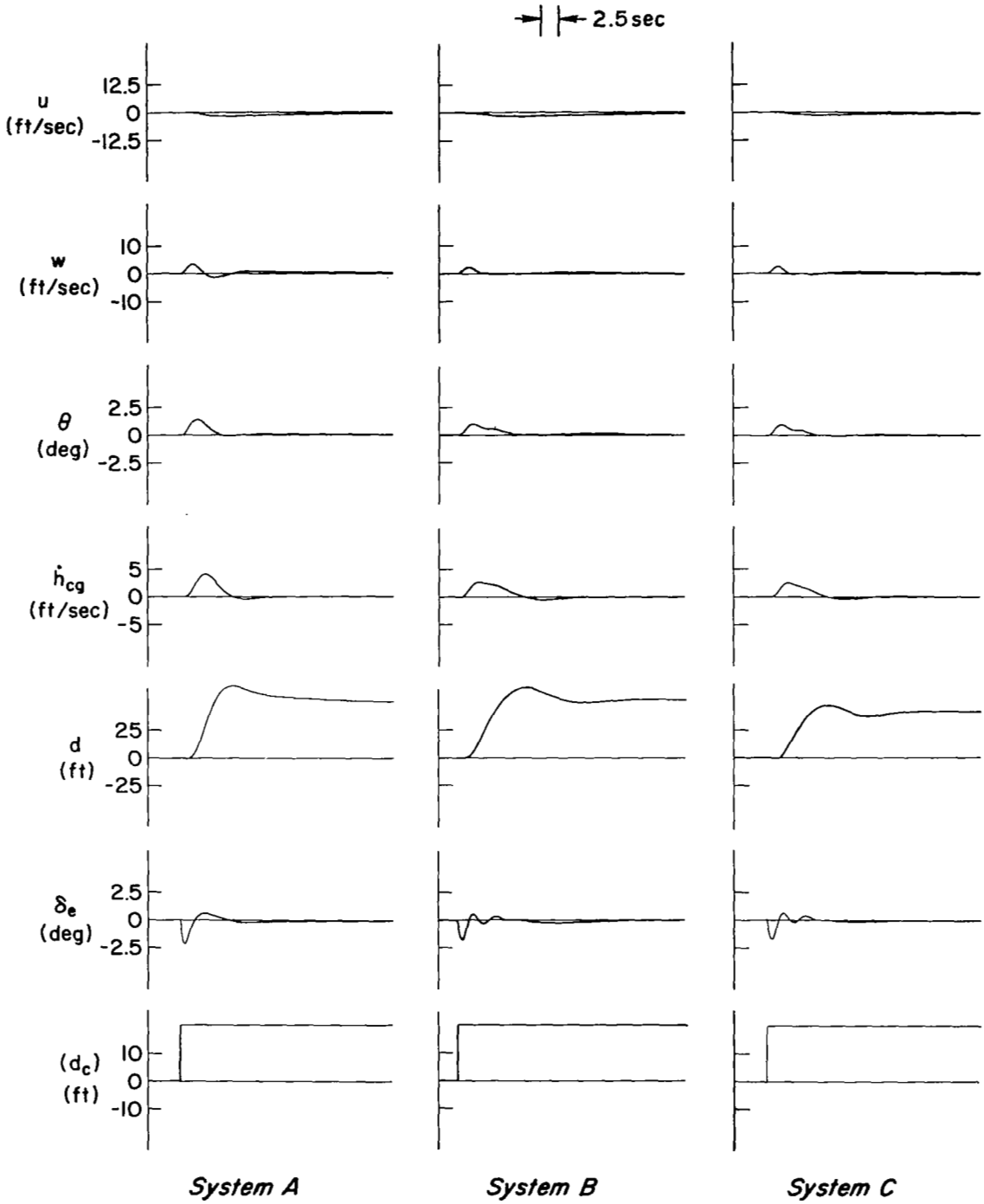

Figure 12. Transient Responses for a Step Deviation Command, d_c

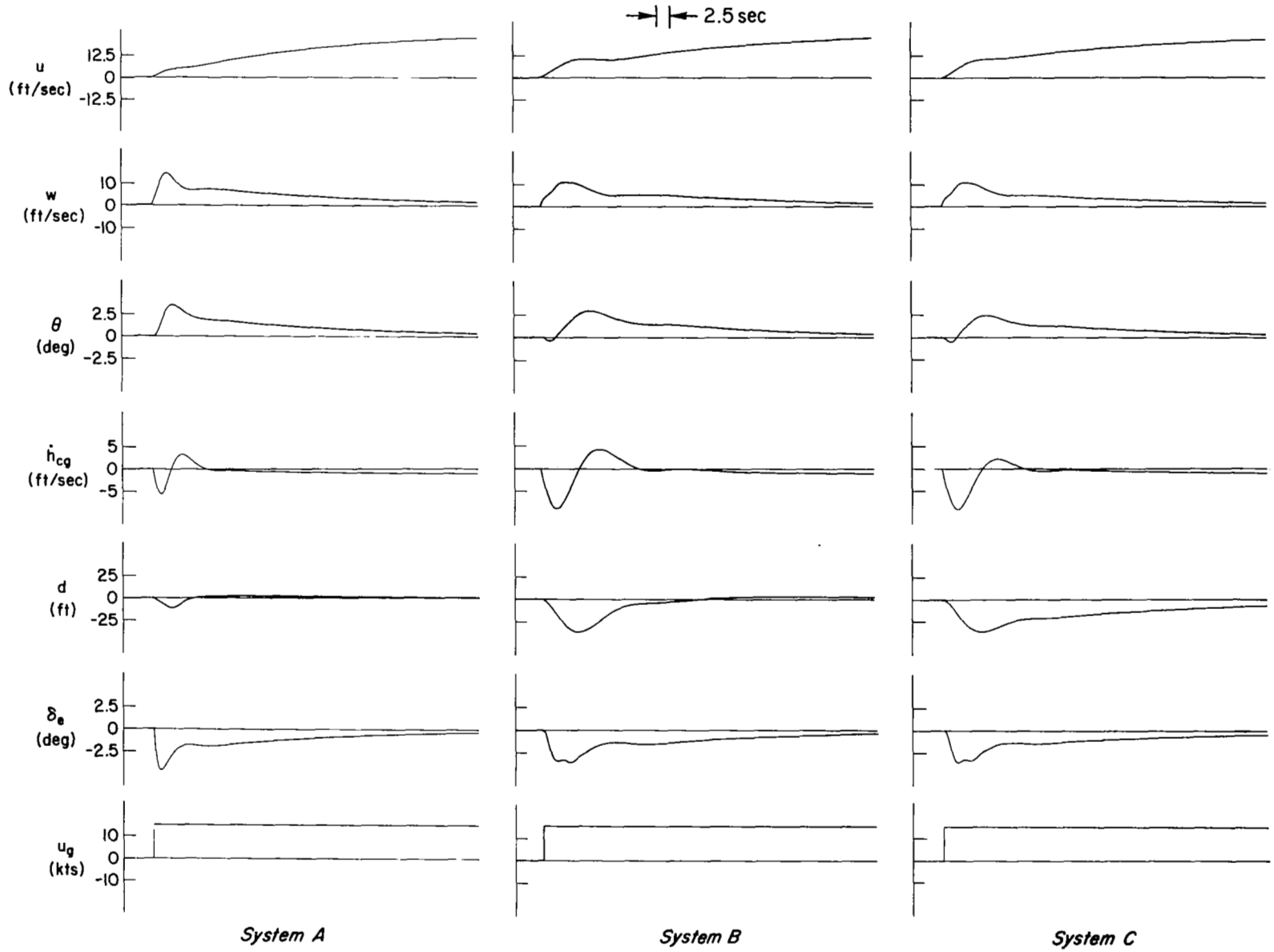

Figure 13. Transient Responses for a Step u_g Gust Input

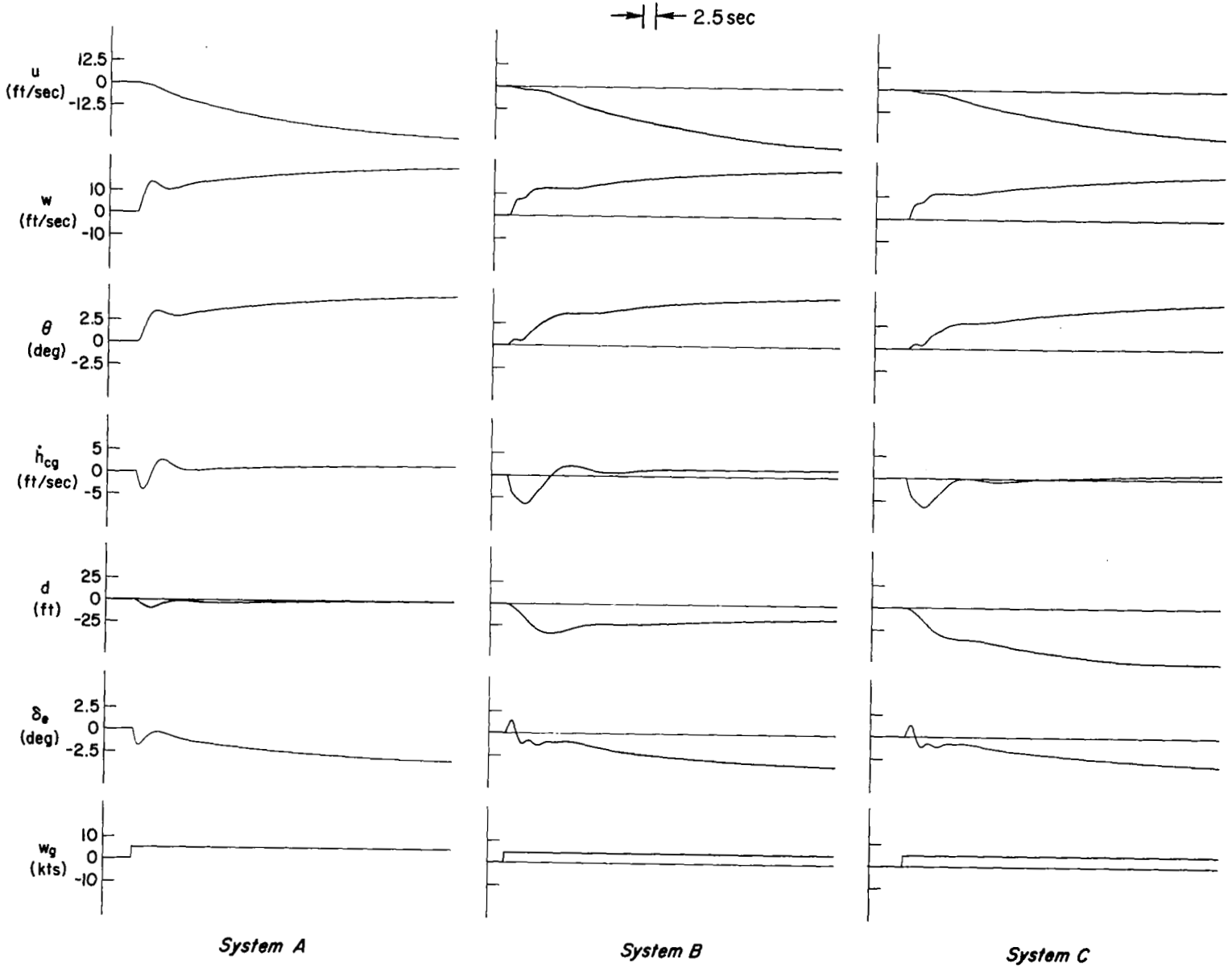

Figure 14. Transient Responses for a Step w_g Gust Input

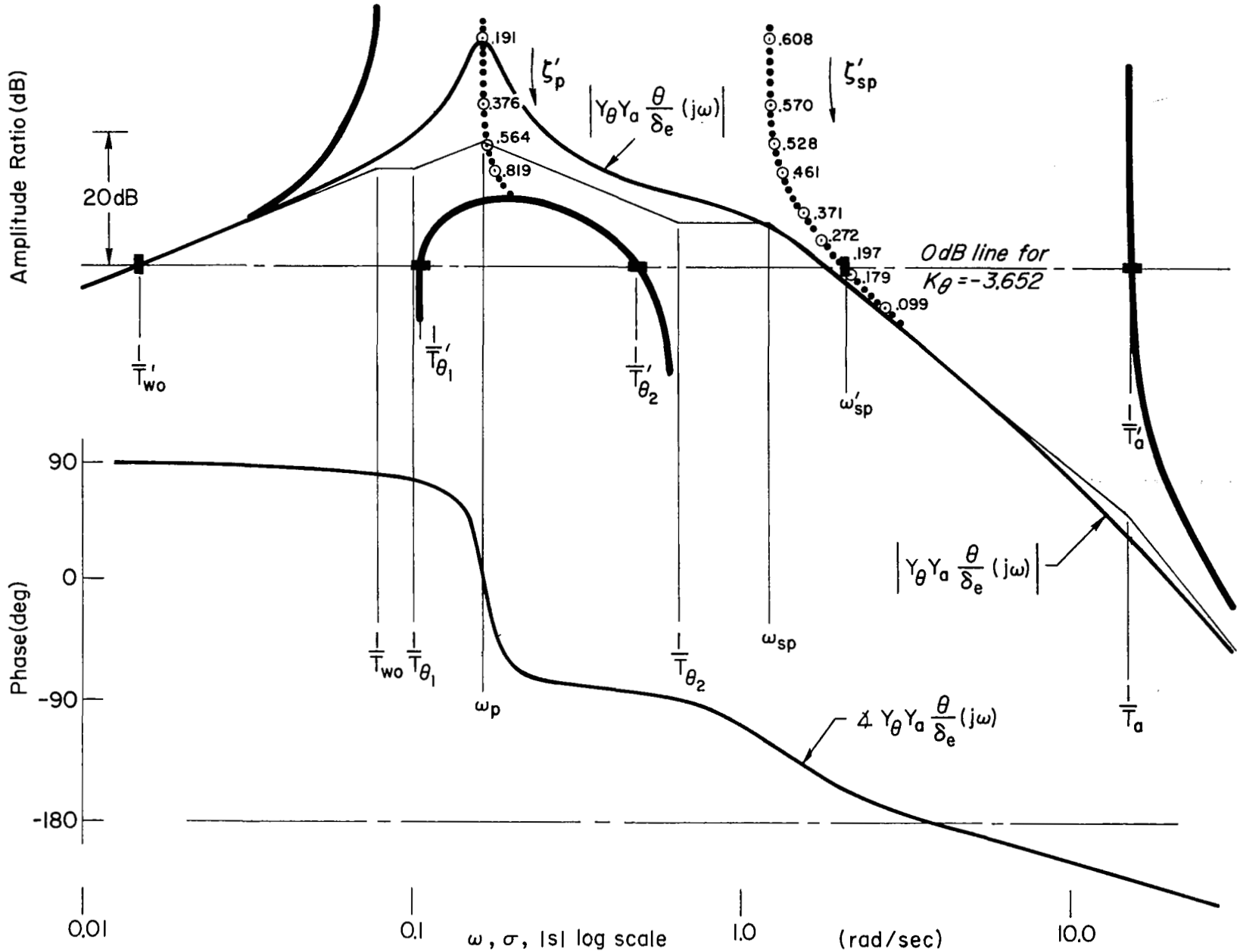

Figure 15. System Survey for Attitude Loop Closure for System B

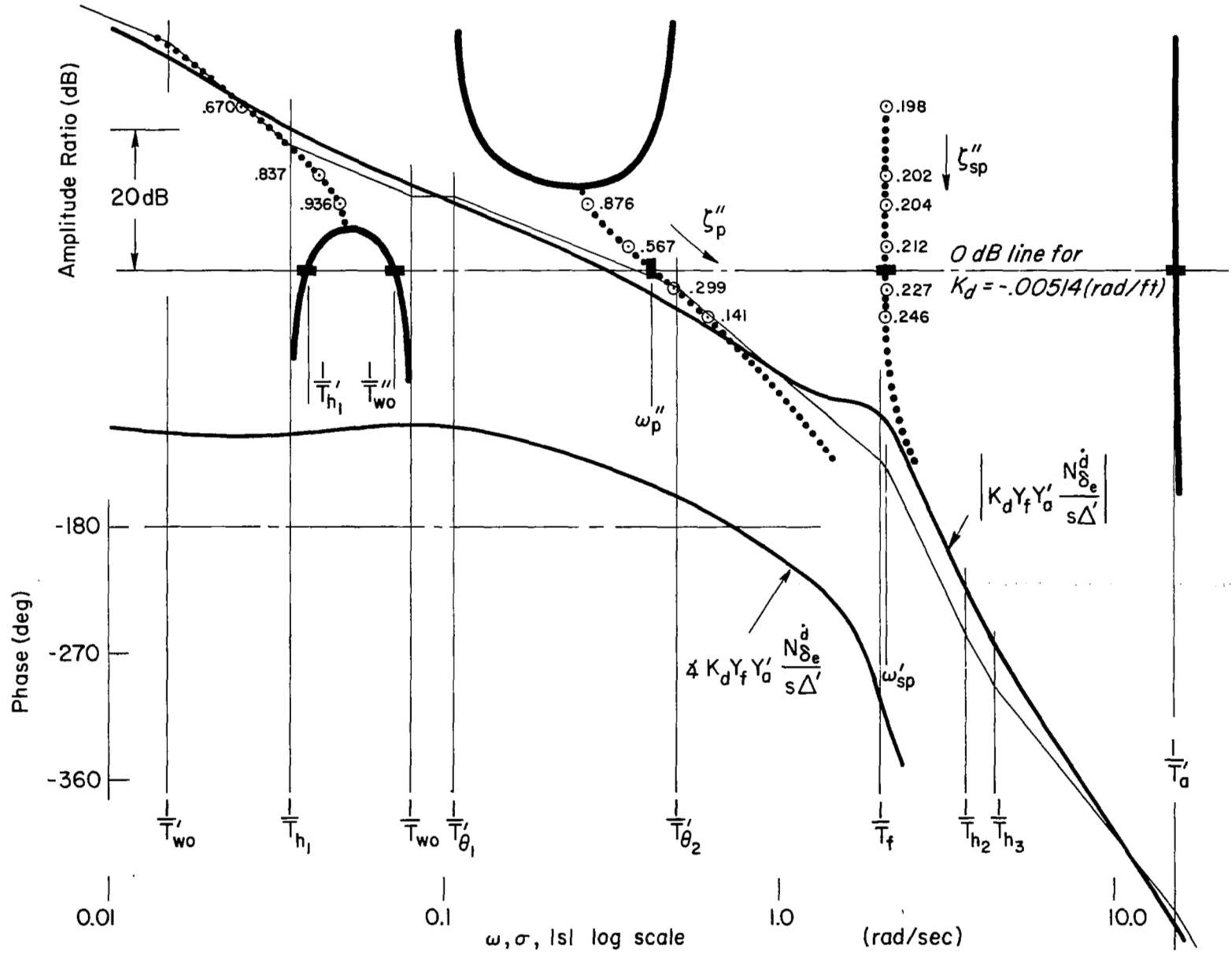

Figure 16. System Survey for Beam Deviation Loop Closure for System B

the crossover frequency. The same deviation-loop gain is used for this system as for the conventional. The closed-loop roots resulting are quite similar to those of System C, although the undamped natural frequency, ω_p'', and damping ratio, ζ_p'', of the dominant mode are slightly less. This is to be expected as a consequence of the introduction of the washout. The closed-loop transfer functions are given in Table 9.

TABLE 9

CLOSED-LOOP TRANSFER FUNCTIONS FOR SYSTEM B

$$\frac{\hat{d}_\epsilon}{u_g} = \frac{+0.566(0)(0.019)(15.23)[0.147\ ,\ 2.099]}{(0.039)(0.07)(2.065)(15.229)[0.424\ ,\ 0.415][0.218\ ,\ 2.06]}$$

$$\frac{\hat{d}_\epsilon}{w_g} = \frac{+1.5(0.015)(0.095)(15.14)[0.309\ ,\ 1.786]}{(0.039)(0.07)(2.065)(15.229)[0.424\ ,\ 0.415][0.218\ ,\ 2.06]}$$

$$\frac{\hat{d}_\epsilon}{d_{command}} = \frac{+2.0(0)(0.018)(0.109)(0.489)(15.229)[0.20\ ,\ 2.07]}{(0.039)(0.07)(2.065)(15.229)[0.424\ ,\ 0.415][0.218\ ,\ 2.06]}$$

$$\frac{u}{u_g} = \frac{0.0373(1.366)(2.167)(15.229)[0.609\ ,\ 0.097][0.191\ ,\ 2.013]}{(0.039)(0.07)(2.065)(15.229)[0.424\ ,\ 0.415][0.218\ ,\ 2.06]}$$

$$\frac{u}{w_g} = \frac{-0.136(0.078)(2.05)(15.225)[-0.241\ ,\ 0.444][0.180\ ,\ 1.978]}{(0.039)(0.07)(2.065)(15.229)[0.424\ ,\ 0.415][0.218\ ,\ 2.06]}$$

$$\frac{u}{d_{command}} = \frac{0.194(0)(0.08)(4.03)(-4.082)}{(0.039)(0.07)(2.065)(15.229)[0.424\ ,\ 0.415][0.218\ ,\ 2.06]}$$

The system transient response characteristics are generally similar to those of System C, with slight variations as expected by the qualitative system differences. The responses to a step d_c command are almost

exactly identical. Some differences would occur, however, if the input were a higher order function, such as a ramp; then the response of System B would be superior. For the w_g step inputs, System B is markedly better than the conventional System C in terms of beam deviation. The other degrees of freedom are generally similar, as would again be expected. Finally, with a u_g step disturbance, System B is again superior in the d response, with the other degrees of freedom again very similar. Thus, in every respect but path deviation loop bandwidth, the modified system (B) is better than the conventional controller (C).

Advanced System (System A)

The advanced system is analytically more complex than the others considered because of the more complicated equalization and because the use of a $K_{\dot{h}}\dot{h}$ signal for path damping requires an additional loop closure. For simplicity of explanation, however, we shall use a $K_{\dot{d}}\dot{d}$ signal rather than a $K_{\dot{h}}\dot{h}$ signal. With this simplifying assumption we can again deal with an attitude and path deviation set of loop closures for the Bode plots. However, it is noted that for the closed-loop analog computer time responses, the actual $K_{\dot{h}}\dot{h}$ signal was used, rather than the simplified $K_{\dot{d}}\dot{d}$ signals.

In the attitude loop, the attitude washout is made somewhat less than the short-period undamped natural frequency so as to assure nearly pure gain attitude feedback at short-period frequency. The addition of the attitude rate signal to the washed out attitude creates a net equalization on θ given by

$$Y_\theta = \frac{K_\theta s}{s + 1/T_{wo}} + K_{\dot{\theta}} s$$

$$= \frac{K_\theta s(s + 1/T_E)}{s + 1/T_{wo}} \qquad (41)$$

where $$\frac{1}{T_E} = \frac{K_\theta}{K_{\dot{\theta}}} + \frac{1}{T_{wo}}$$

The location of the lead equalization breakpoint, $1/T_E$, is the primary means to adjust the short-period damping ratio. If this breakpoint is placed somewhat greater than ω_{sp}, a long stretch of −20 dB per decade slope will be established between $1/T_E$ and the actuator breakpoint at $1/T_a$. Gain crossover anywhere in this stretch will result in reasonable damping of the short-period mode, while still permitting reasonably large amplitude ratio values at mid-frequencies. This is illustrated in the attitude control jω Bode and Bode root-locus in Fig. 17. There, it is seen that with an increase in gain the phugoid and short-period damping ratios, and the short-period undamped natural frequency are all increased, while the phugoid undamped natural frequency is decreased. The physical explanation for the decrease of phugoid frequency with System A is the significantly lower amplitude ratio of the θ feedback at phugoid frequency (compared to System B), which is due to the difference in the washout time constants.

Consider now the beam deviation closure. Here, the equalization, Y_d, has both a rate and integral term in addition to the glide-slope-beam noise filter, i.e.,

$$Y_d = \frac{K_{\bar{d}} + K_d s}{s(T_f s + 1)} + K_{\dot{d}} s$$

$$= \frac{K_{\dot{d}}[s^3 + (1/T_f)s^2 + (K_d/T_f K_{\dot{d}})s + K_{\bar{d}}/T_f K_{\dot{d}}]}{s(s + 1/T_f)}$$

$$= \frac{K_{\dot{d}}(s + 1/T_{d_1})(s + 1/T_{d_2})(s + 1/T_{d_3})}{s(s + 1/T_f)}$$

where $$\frac{1}{T_{d_1}} \doteq \frac{K_{\bar{d}}}{K_d}, \quad \frac{1}{T_{d_2}} \doteq \frac{K_d}{K_{\dot{d}}}, \quad \frac{1}{T_{d_3}} \doteq \frac{1}{T_f}$$

At very low frequencies, the open-loop system looks like K/s^2 because of the integral term in the deviation controller. The rest of the equalization is needed to adjust the amplitude ratio to approximate a −20 dB per decade slope in the desired region of crossover. While Y_d has three time constants, $1/T_{d_3}$ is inherently close to the beam noise filter breakpoint,

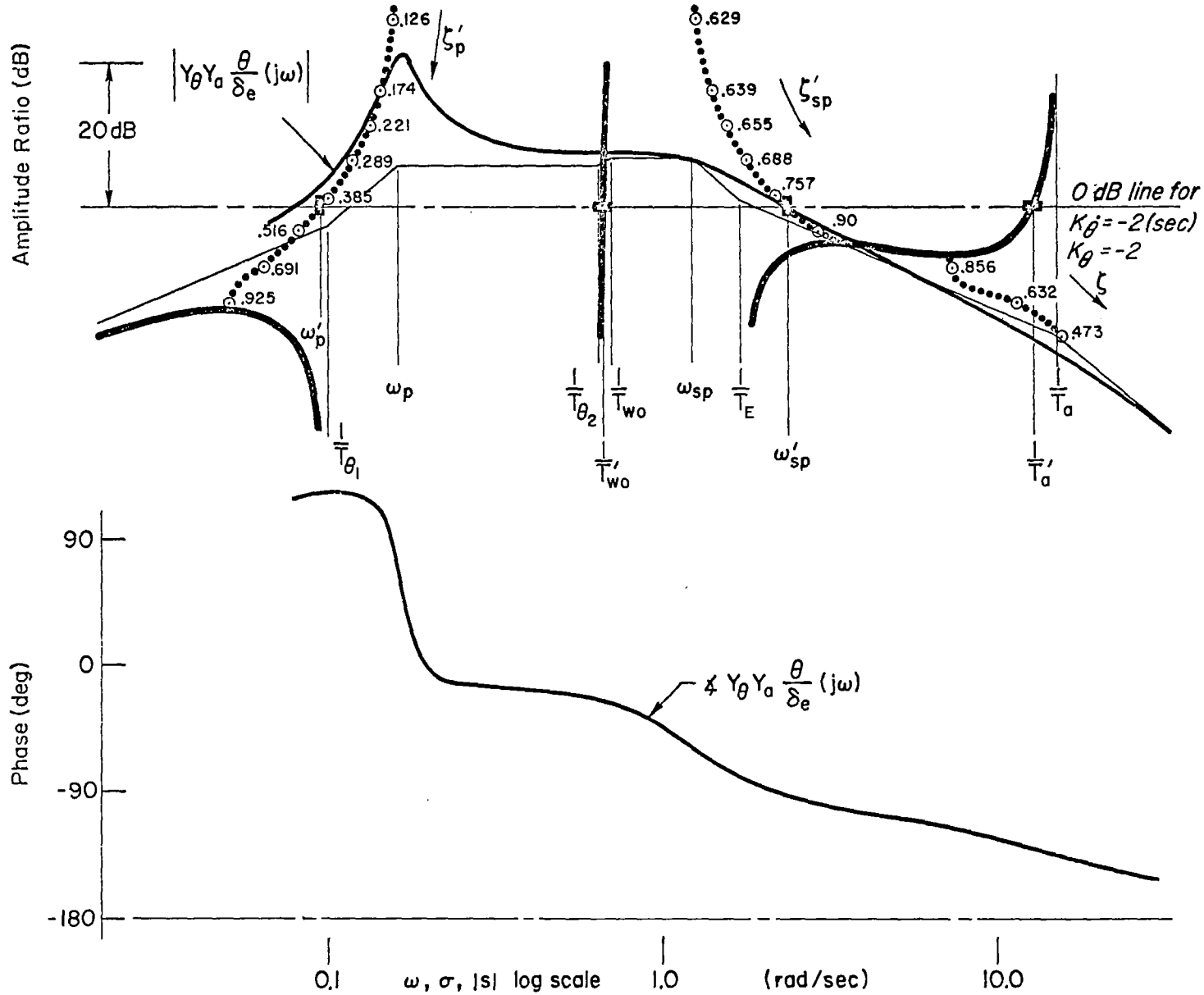

Figure 17. System Survey for Attitude Loop Closure for System A

so the best that can be achieved is to create a dipole pair near $1/T_f$ giving a small phase lead in the region of the filter. The principal adjustments are then $1/T_{d_1}$ and $1/T_{d_2}$. When these breakpoints are positioned relative to the ω_p' breakpoint, as shown in Fig. 18, the low-frequency amplitude ratio attainable with a given zero dB line is made as large as possible. However, note that the phase in the low-to-medium frequency region must not be permitted to exceed -180°. This is important for avoiding a low-frequency, low-amplitude oscillation due to any system threshold or hysteresis characteristics (either of these will result in reduced gain at very low amplitudes which could set the conditions for a limit cycle at a frequency where the phase angle reaches -180°). If the loops are closed with the gains noted, then a crossover frequency corresponding to a maximum attainable phase margin of about 32° is achieved. The resulting closed-loop characteristics are greatly superior to those of either the conventional or modified system in bandwidth, path following, dominant and short-period mode characteristics, etc. The closed-loop transfer functions are given in Table 10.

The general superiority of System A is also exhibited in the transient response comparisons of Figs. 12 through 14. Deviation responses for both command and disturbance inputs are all superior, as are all the degrees of freedom which most strongly reflect short-period properties. A summary table of the various control system constants is given in Table 11 for easy reference.

The speed responses are very similar for all three systems. This reflects the lack of a speed control loop. The basic time-constant of the speed deviation is limited by $1/T_{h_1}$. In terms of approximate factors, this is given by

$$\frac{1}{T_{h_1}} \doteq -X_u + (X_\alpha - g)\frac{Z_u}{Z_\alpha}\frac{(1 - Z_{\delta_e}M_u/M_{\delta_e}Z_u)}{(1 - Z_{\delta_e}M_\alpha/M_{\delta_e}Z_\alpha)} \qquad (42)$$

When a speed-control system is considered as a stability augmenter, an α or u to δ_t feedback will modify X_u or X_α, and thus can be used to change

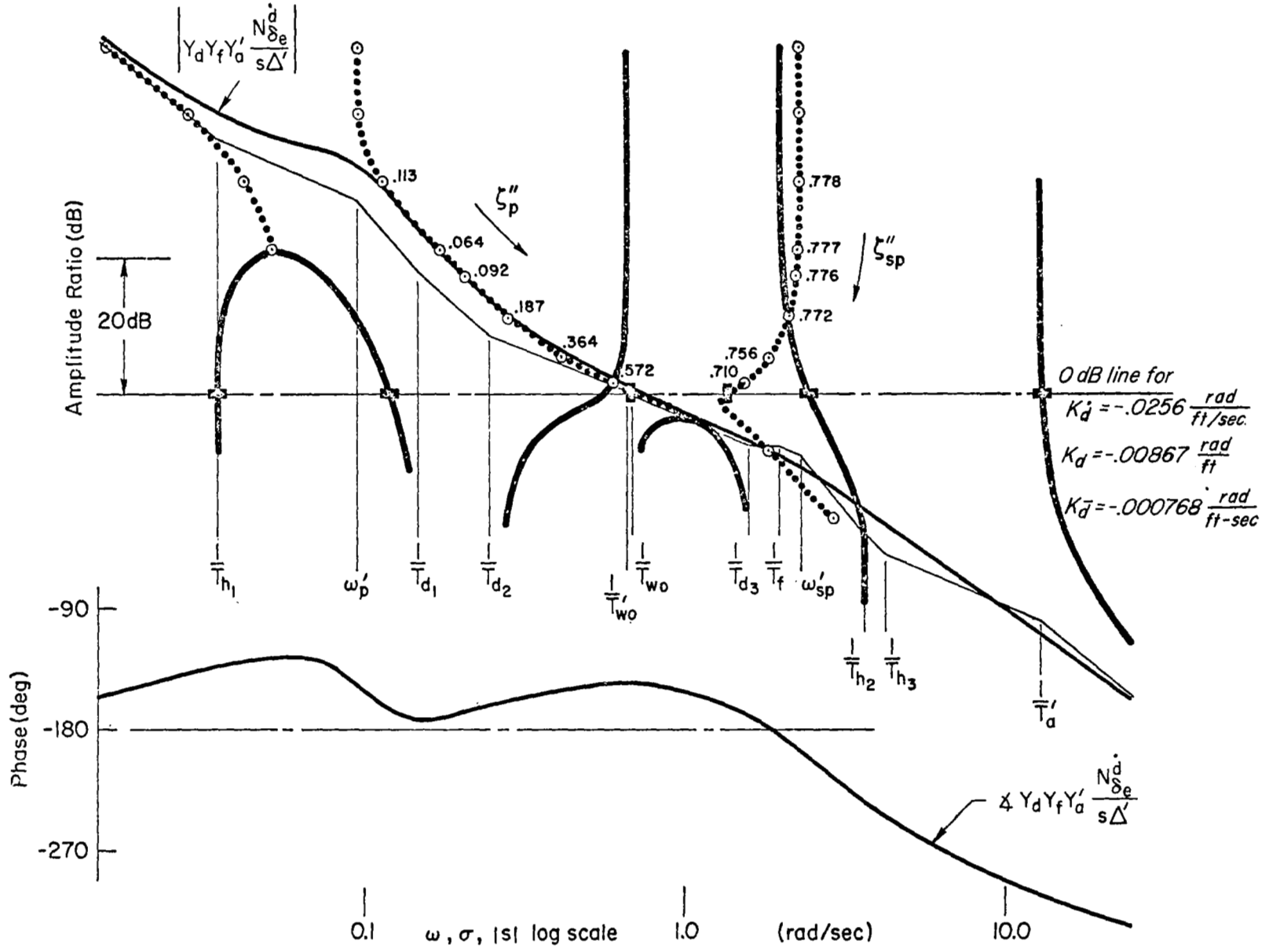

Figure 18. System Survey for Beam Deviation Loop Closure for System A

$1/T_{h_1}$. Then the deviation loop closure will result in a larger value of $1/T'_{h_1}$, with a concomitant improvement in the closed-loop system speed response in all three systems.

TABLE 10

CLOSED-LOOP TRANSFER FUNCTIONS FOR SYSTEM A

$$\frac{\hat{d}_\epsilon}{u_g} = \frac{+0.566(0)(0)(0.174)(12.918)[0.767\ ,\ 2.215]}{(0.036)(0.123)(0.582)(2.462)(13.232)[0.657\ ,\ 0.699][0.673\ ,\ 1.428]}$$

$$\frac{\hat{d}_\epsilon}{w_g} = \frac{+1.5(0)(13.75)[0.464\ ,\ 0.103][0.936\ ,\ 2.018]}{(0.036)(0.123)(0.582)(2.462)(13.232)[0.657\ ,\ 0.699][0.673\ ,\ 1.428]}$$

$$\frac{\hat{d}_\epsilon}{d_{command}} = \frac{+2.0(0)^2(0.044)(0.733)(2.0)(13.22)[0.43\ ,\ 1.46]}{(0.036)(0.123)(0.582)(2.462)(13.232)[0.657\ ,\ 0.699][0.673\ ,\ 1.428]}$$

$$\frac{u}{u_g} = \frac{-0.0373(0.136)(1.596)(2.777)(13.261)[0.5\ ,\ 0.276][0.58\ ,\ 1.918]}{(0.036)(0.123)(0.582)(2.462)(13.232)[0.657\ ,\ 0.699][0.673\ ,\ 1.428]}$$

$$\frac{u}{w_g} = \frac{-0.136(0.153)(0.215)(2.409)(13.262)[-0.082\ ,\ 1.023][0.872\ ,\ 1.492]}{(0.036)(0.123)(0.582)(2.462)(13.232)[0.657\ ,\ 0.699][0.673\ ,\ 1.428]}$$

$$\frac{u}{d_{command}} = \frac{0.3272(0)(0.089)(0.7)(-4.082)(4.03)}{(0.036)(0.123)(0.582)(2.462)(13.232)[0.657\ ,\ 0.699][0.673\ ,\ 1.428]}$$

TABLE 11

SUMMARY OF CONTROL SYSTEM CONSTANTS

	A	B	C
K_θ	−2.	−3.652	−3.652
$K_{\dot{\theta}}$ (sec)	−2.	0	0
$K_{\dot{d}}$ (rad-sec/ft)	−0.0256	0	0
K_d (rad/ft)	−0.00867	−0.00514	−0.00514
$K_{\overline{d}}$ (rad/ft-sec)	−0.000768	0	0
$1/T_{wo}$ (1/sec)	0.7	0.08	0
$1/T_a$ (1/sec)	15.	15.	15.
$1/T_f$ (1/sec)	2.	2.	2.

REFERENCES

1. Johnson, Walter A., and Duane T. McRuer, Development of a Category II Approach System Model, Systems Technology, Inc., Tech. Rept. 182-2, Oct. 1970. NASA CR-2022.

2. McRuer, Duane, Irving Ashkenas, and Dunstan Graham, Aircraft Dynamics and Automatic Control, Princeton University Press, 1972.

NASA-Langley, 1972 —— 21